



OPEN ACCESS

EDITED BY

Sergey Alexander Pulinets,
Space Research Institute (RAS), Russia

REVIEWED BY

Yasuhide Hobara,
The University of Electro-
Communications, Japan
Yenca Migoya Orué,
The Abdus Salam International Centre
for Theoretical Physics (ICTP), Italy

*CORRESPONDENCE

Veronika Barta,
bartav@ggki.hu

SPECIALTY SECTION

This article was submitted to
Atmosphere and Climate,
a section of the journal
Frontiers in Environmental Science

RECEIVED 25 March 2022

ACCEPTED 30 June 2022

PUBLISHED 26 August 2022

CITATION

Barta V, Natras R, Srećković V,
Koronczay D, Schmidt M and Šulic D
(2022), Multi-instrumental investigation
of the solar flares impact on the
ionosphere on 05–06 December 2006.
Front. Environ. Sci. 10:904335.
doi: 10.3389/fenvs.2022.904335

COPYRIGHT

© 2022 Barta, Natras, Srećković,
Koronczay, Schmidt and Šulic. This is an
open-access article distributed under
the terms of the [Creative Commons
Attribution License \(CC BY\)](https://creativecommons.org/licenses/by/4.0/). The use,
distribution or reproduction in other
forums is permitted, provided the
original author(s) and the copyright
owner(s) are credited and that the
original publication in this journal is
cited, in accordance with accepted
academic practice. No use, distribution
or reproduction is permitted which does
not comply with these terms.

Multi-instrumental investigation of the solar flares impact on the ionosphere on 05–06 December 2006

Veronika Barta^{1*}, Randa Natras², Vladimir Srećković³,
David Koronczay^{1,4}, Michael Schmidt² and Desanka Šulic⁵

¹Institute of Earth Physics and Space Science (ELKH EPSS), Sopron, Hungary, ²Department of Geodesy and Aerospace, Deutsches Geodätisches Forschungsinstitut der Technischen Universität München (DGF-I-TUM), Technical University of Munich, Munich, Germany, ³Institute of Physics Belgrade, University of Belgrade, Belgrade, Serbia, ⁴Department of Geophysics and Space Science, Institute of Geography and Earth Sciences Eötvös Loránd University, Budapest, Hungary, ⁵Faculty of Ecology and Environmental Protection, University Union - Nikola Tesla, Belgrade, Serbia

The sudden increase of X-radiation and EUV emission following solar flares causes additional ionization and increased absorption of electromagnetic (EM) waves in the Earth's atmosphere. The solar flare impact on the ionosphere above Europe on 05 and 06 December 2006 was investigated using ground-based (ionosonde and VLF) and satellite-based data (Vertical Total Electron Content (VTEC) derived from GNSS observations and VLF measurements from DEMETER satellite). Based on the Kp and Dst indices, 05 December 2006 was a quiet day, while there was a geomagnetic storm on 06 December 2006. The total fade-out of the EM waves emitted by the ionosondes was experienced at all investigated stations during an X9 class flare on 05 December 2006. The variation of the fmin parameter (first echo trace observed on ionograms, it is a rough measure of the "non-deviative" absorption) and its difference between the quiet period and during the flares have been analyzed. A latitude dependent enhancement of fmin (2–9 MHz) and Δf_{min} (relative change of about 150%–300%) was observed at every station at the time of the X9 (on 05 December) and M6 (on 06 December) flares. Furthermore, we analyzed VTEC changes during and after the flare events with respect to the mean VTEC values of reference quiet days. During the X9 solar flare, VTEC increased depending on the latitude (2–3 TECU and 5%–20%). On 06 December 2006, the geomagnetic storm increased ionization (5–10 TECU) representing a "positive" ionospheric storm. However, an additional peak in VTEC related to the M6 flare could not be detected. We have also observed a quantifiable change in transionospheric VLF absorption of signals from ground transmitters detected in low Earth orbit associated with the X9 and M6 flare events on 05 and 06 December in the DEMETER data. Moreover, amplitude and phase of ground-based, subionospherically propagating VLF signals were measured simultaneously during the investigated flares to analyze ionosphere reaction and to evaluate the electron density profile versus altitude. For the X9 and M6 flare events we have also calculated the ionospheric parameters (sharpness, reflection height) important for the description and modelling of this medium under forced additional ionization.

KEYWORDS

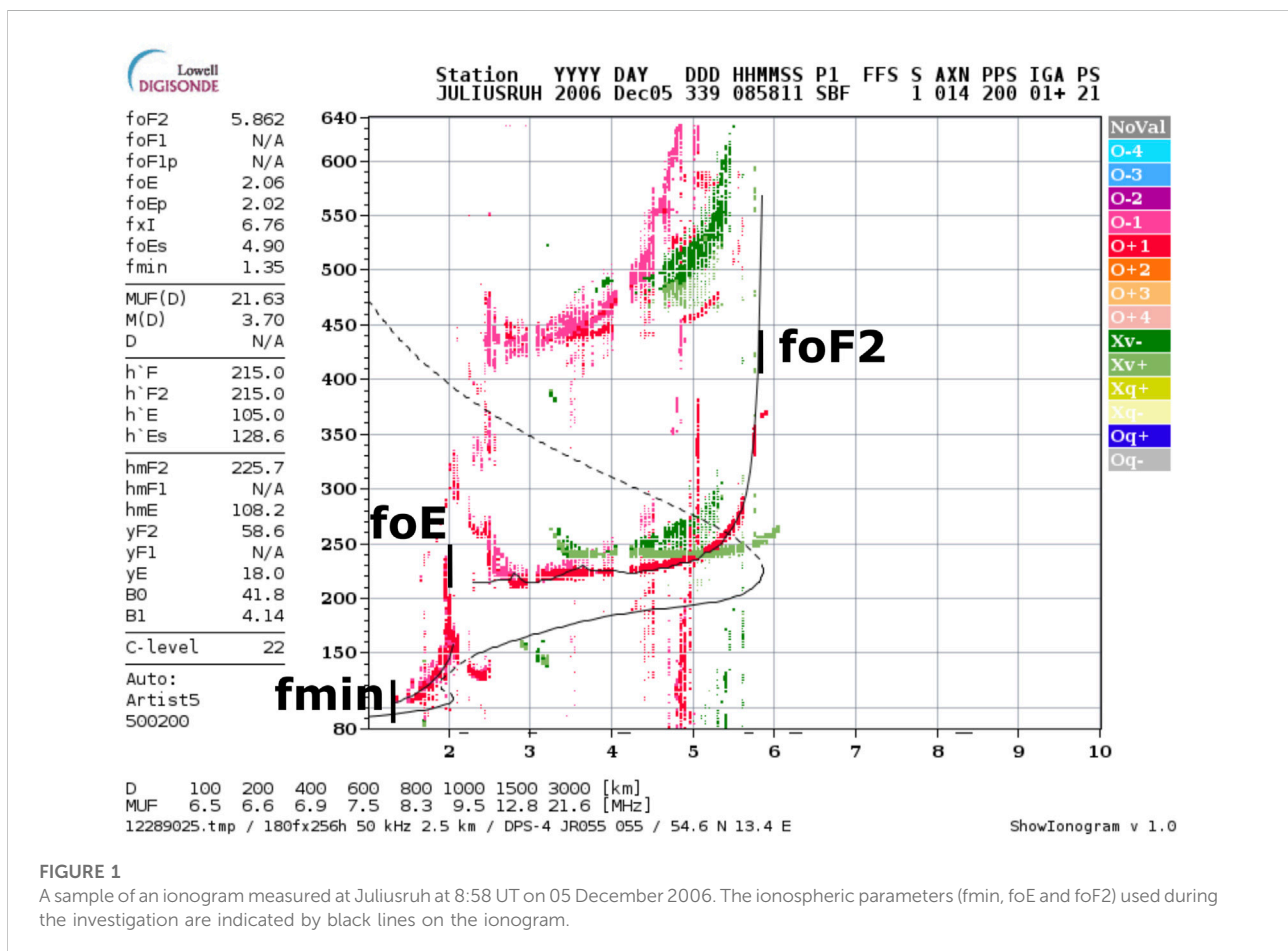
space weather, solar flare, ionosphere, observations, ionosonde data, total electron content, very low frequency signals

1 Introduction

Solar flares are known to cause enhanced ionization on the Earth's atmosphere in the sunlit hemisphere (Davies, 1990; Pröls 2004; Tsurutani et al., 2009). Solar flares are giant explosions on the surface of the Sun when a huge amount of electromagnetic energy is released over the whole electromagnetic spectrum. When energy from a solar flare reaches Earth, the ionosphere becomes suddenly more ionized, thus changing the density and location of layers. Hence the term Sudden Ionospheric Disturbance, SID is used to describe the changes of the ionosphere. Enhanced EUV radiation is absorbed at higher altitudes ionizing the E and F regions of the ionosphere (e.g., Tsurutani et al., 2005; Manju et al., 2009). X-rays penetrate more deeply into the ionosphere reaching the D region and causing enhanced ionization and absorption of the EM waves there (Davies, 1990; Sripathi et al., 2013). Solar flares can potentially affect

space-based communication and navigation systems and cause short radio wave blackout.

A 1 h period lack of traces on the ionograms was detected over the Brazilian sector during the 28 October 2003 flare event (Sahai et al., 2007). The total radio blackout was explained by the enhanced ionospheric absorption. Sripathi et al. (2013) also observed lack of echo on the ionograms simultaneously with an amplified signal amplitude in VLF records during an intense (X7) flare. They explained the detected variations by the enhanced ionization and HF radio wave absorption in the D region. Denardini et al. (2016) also detected partial radio fade-out (below 5–8 MHz) on the ionograms which they attributed to enhanced X-ray ionization due to solar flares. The f_{min} parameter (minimum frequency of reflection on the ionograms, see Figure 1.) were used in several studies to investigate the ionospheric response to solar flares. This parameter is usually considered as a rough measure of the “non-deviative” radio wave absorption in the ionosphere



(Rishbeth and Garriot, 1969; Davies, 1990). Enhanced values of the f_{min} and a ~70 min long total radio fade-out were observed at two low-latitude ionosonde stations with a consistent time difference in the onset and the recovery (Nogueira et al., 2015). The authors stated that the reason for this time delay was the east-west separation of the two observation sites. Barta et al. (2019) reported total radio blackout with varying duration (15–150 min) and enhanced values of the f_{min} parameter measured at different low- and midlatitude stations during M and X class solar flares. The changes detected in the f_{min} were highly dependent on the X-ray flux, but they also depended on the solar zenith angle of the observation site.

Observations from Global Navigation Satellite Systems (GNSS) provide a possibility to estimate the total number of free electrons (Total Electron Content or TEC) along the signal's ray path between the satellite and the receiver. TEC is related to the GNSS signal propagation delay to the ionosphere. The global study of X57 solar flare effect (14 July 2000) on the ionosphere by means of vertical TEC (VTEC) showed that the ionospheric VTEC response depends mainly on local time, where the most pronounced solar flare effects were visible during mid-day (Liu et al., 2004). Also, other studies reported a connection between the enhanced ionization in the daylight hemisphere and solar zenith angle (Hernandez-Pajares et al., 2012; Xiong et al., 2014). Thus the most pronounced VTEC changes due to strong solar flares can be expected around local noon when the solar zenith angle is close to zero. On 05 December 2006, the TEC increase of about 4 TECU was reported from a GPS receiver located at Ascension Island (low latitude region) during an X9.0 solar flare (Carrano et al., 2009). Strong solar flares can also cause solar radio bursts. On 06 December 2006, the solar radio burst affected the reception of GPS (Global Positioning Service) signals and degraded GPS availability and positioning accuracy on the sunlit hemisphere during an X6.0 solar flare (Cerruti et al., 2008). In September 2017, a solar radio burst resulting from an X9.3 solar flare affected the GNSS positioning performance and navigation services in Europe (Berdermann et al., 2018). Also, a high number of solar flares of classes X and M in October 2014 produced enhanced ionization in the mid-latitude ionosphere over the south-east of Europe and degraded GNSS precise point positioning (Natras et al., 2019).

The Very Low Frequency (VLF, 3–30 kHz) is below the critical frequencies, i.e., plasma frequencies of the ionospheric D region plasma (Davies, 1965). Consequently, VLF radio signals propagate from transmitters within the waveguide created by the low ionosphere (the D region, $50 \leq h \leq 90$ km) and Earth's surface (see e.g., Wait and Spies 1964; Mitra 1974; Kelley 2009). VLF radio signal propagation is normally characterized by good stability, especially by day and has low path attenuation (Folkestad, 2013). VLF radio waves reflect from ionospheric layers at altitudes of 70–75 km during

daytime and 80–90 km during nighttime while the effective reflection height depends on the level of ionization of the D-region (Budden, 1961). SID are followed by variations in electron density of the lower ionosphere, which affect the subionospheric VLF radio signal propagation as a deviation in amplitude A and/or phase φ (Goodman 2005). As it can be seen from literature (see e.g., Grubor et al., 2008), VLF radio signal amplitude and phase perturbations are in correlation with the strength of sudden X-ray irradiance. In previous studies sudden X-ray irradiance (flares of class X, M, even C) induced absolute increase of the amplitude and phase of VLF recordings (Thomson and Clilverd 2001; Šulić et al., 2016) and in some cases showed almost monotonous logarithmic increase of ΔA with the solar X-ray irradiance (Žigman et al., 2007; Šulić and Srećković 2014). During the appearance of solar flares, classified as a minor B and small flare (up to the C2 class), the VLF radio signal usually does not have significant perturbations. However, in some cases, data can be also useful for further analysis and calculations of ionospheric parameters (see Raulin et al., 2010; Šulić and Srećković 2014). Here the study of ground based VLF data was done simultaneously with the analysis of the corresponding solar X-ray energy during December 2006. The intensity of the received VLF radio signal changes accordingly to the degree of ionization during the event of a solar flare, i.e., the size of VLF radio signal perturbations is in correlation with the intensity of X-ray irradiance. The ionospheric parameters were calculated using the method developed and elaborated by Grubor et al. (2008), Žigman et al. (2007), and Šulić et al. (2016).

While VLF waves propagate in Earth-ionosphere waveguide with low path attenuation, an attenuated fraction can cross the ionosphere and may propagate further into the plasmasphere surrounding Earth. The resulting radiation pattern at altitudes corresponding to low Earth orbit have been observed in long-term analyses of the electric and magnetic field data recorded by the DEMETER satellite between 2004 and 2011 (Cohen and Inan, 2012; Greninger 2016; Koronczay et al., 2018). In the present study, we look at individual satellite passes of DEMETER close to such ground transmitters at just the right time to observe the attenuation of the trans-ionospheric VLF signals due to solar flare caused enhancement.

The listed observational techniques (TEC, ionosonde data, ground and satellite based VLF method) can reflect ionospheric response to solar flares in different ways whereas they are sensitive to the changes occurring at different heights. Most studies are limited to a single or only some stations of a certain observational method (using mostly VLF or TEC data). However, data of a single station can reflect only the local but not regional or global changes. Furthermore, data obtained from different latitudes can differ considerably. Generally, studies in the literature investigate the ionospheric changes caused by solar flare from the perspective of one

observational technique. However, a single type of data cannot represent the overall response of the ionosphere to solar flares. The number of comprehensive studies using different detection methods are very limited (e.g., Sripathi et al., 2013; Feng et al., 2021).

The aim of the present study is to investigate the solar flare effects on the sunlit hemisphere of the ionosphere focusing on the changes that occurred above the European region (mid-latitude) on 05 and 06 December 2006. Ionosonde data, ground-based VLF measurements, GNSS-derived VTEC and VLF measurements of the DEMETER spacecraft were used in the present research. Comprehensive analysis of the ionospheric response to solar flares measured by the different methods have been performed. Therefore, we determined sensitivity differences between the different observational techniques. The paper is structured as follows: in Section 2 we describe the used observational methods and data; in Section 3 we present the results obtained by the different techniques; in Section 4 we discuss the findings of the investigation while in Section 5 conclusions are presented.

2 Methods and data

Four flare events were chosen for the investigation. They occurred at 08:03 UT (class: M1.8, start: 7:45 UT, end:8:06 UT); at 10:35 UT (class: X9.0, start: 10:18 UT, end: 10:45 UT) on 05 December and at 08:23 UT (class: M6, start: 8:02 UT, end: 9:03 UT); at 12:58 UT (class: C4.8, start: 12:53 UT, end: 13:03 UT) on 06 December 2006. The data from the GOES 11 and 12 satellites used to investigate the X-ray and solar proton flux were available at the OmniWeb database (<https://omniweb.gsfc.nasa.gov/>).

2.1 Ionosonde data

We analyzed the time series of the f_{min} parameter (see Figure 1) inferred from ionograms during the solar flares on 05 and 06 December 2006. To minimize and compensate the instrumental errors, data measured by Lowell type digisondes [Global Ionospheric Radio Observatory (GIRO, <http://giro.uml.edu>) data] was used for the analyses because the f_{min} parameter can also depend on the radar characteristics and the radio-noise level. Furthermore, a df_{min} parameter (the difference between the value of the f_{min} and the mean f_{min} for reference days: $f_{min_{flare}} - f_{min_{quiet}}$) have also been defined for the investigation. The reference period (16–27 November 2006 and 28 December 2006–09 January 2007) has been selected based on the X-ray radiation ($<0.5 \cdot 10^{-4}$) and proton flux [0.8–4 MeV] ($<3 \cdot 10^3$) measured by GOES satellites. In order to draw a parallel between the observed changes measured by the different instruments (e.g., TEC variation, or N_e variation based on VLF records) the

residuals (relative changes in percentage compared to the reference days) has also been determined using the following equation:

$$\Delta f_{min} = \frac{f_{min_{flare}} - f_{min_{quiet}}}{f_{min_{quiet}}} \cdot 100 \quad (1)$$

This formula is regularly used in the analysis of the foF2 parameter during geomagnetic storms in the literature (e.g., Buresova et al., 2014; Berényi et al., 2018):

$$\Delta foF2 = \frac{foF2_{storm} - foF2_{quiet}}{foF2_{quiet}} \cdot 100 \quad (2)$$

Moreover, the variation of the foE and foF2 parameters (Figure 1) have also been analyzed during the investigated period. The ionograms have been manually verified and evaluated before the analysis. The investigation has been repeated for ionospheric data recorded at European and South-African ionosonde stations at different latitudes (thus under different solar zenith angles at the time of the selected flare events, Table 1 and Figure 2). The ionograms used for the analysis were derived from the Global Ionospheric Radio Observatory network (GIRO, <http://giro.uml.edu>) and were processed by the SAO-X program.

2.2 Vertical total electron content estimation from GNSS measurements

Slant Total Electron Content (STEC) represents the integrated electron density along the GNSS signal path from the satellite s to the receiver r as

$$STEC = \int_r^s N_e ds \quad (3)$$

where N_e represents the electron density. Using a mapping function, which depends on the elevation, and approximating the ionosphere with single layer model (SLM) (Schaer, 1999), STEC can be mapped into VTEC as

$$VTEC = STEC \cos \left[\sin^{-1} \left(\frac{R \cos \theta}{R + H} \right) \right] \quad (4)$$

where H is a mean altitude of the SLM, R stands for mean Earth radius, θ is the elevation angle at the receiver. SLM assumes that all free electrons are concentrated in a single ionospheric shell of infinitesimal thickness at H . The SLM height typically ranges between 350 and 450 km (Mannucci et al., 1998; Schaer, 1999; Jiang et al., 2017).

Carrier phase GNSS measurements of GPS and GLONASS were used to estimate STEC. A calibration of STEC was performed following the methodology by Ciruolo et al. (2007) with a sampling rate of the 30 s. STEC was estimated for all visible satellites applying an elevation mask of 10° . STEC is converted to

TABLE 1 The name, location and geographical coordinates of the stations used in this study. The transmitter frequency of the VLF stations are in brackets after the name of the station. The GCP for the ground-based VLF measurements are: 1,980 km for the GQD-BEL path and 11,980 km for the NWC-BEL path.

Name and geographical coordinates of the stations

Name of station	City	Country	Latitude [°]	Longitude [°]
Ionosonde stations				
JR055	Juliusruh	Germany	54.60	13.40
PQ052	Pruhonicé	Czechia	50.00	14.60
RO041	Rome	Italy	41.90	12.50
VT139	San Vito	Italy	40.60	17.80
AS00Q	Ascension Island	United Kingdom	-7.95	345.60
MU12K	Madimbo	South Africa	-22.38	30.88
GR13L	Grahamstown	South Africa	-33.30	26.50
GNSS stations				
BUDP	Kobenhavn	Denmark	55.74	12.50
KUNZ	Kunzák	Czechia	49.11	15.20
AQUI	L'Aquila	Italy	42.37	13.35
MATE	Matera	Italy	40.65	16.70
VLF transmitters observed by the DEMETER				
DHO (23.40 kHz)	Rhauderfehn	Germany	53.08	7.62
HWV (21.57 kHz)	St. Assise	France	48.54	2.57
GBZ (19.60 kHz)	Anthorn	United Kingdom	54.91	-3.27
ICV (20.27 kHz)	Isola di Tavolara	Italy	40.88	9.68
Receiver station for ground-based VLF measurements and transmitters				
AbsPAL system	Belgrade	Serbia	44.85	20.38
NWC (19.80 kHz)	H. E. Holt	Australia	-21.80	114.15
GQD (22.10 kHz)	Skelton	United Kingdom	54.73	-2.88

VTEC by applying Eq. 4, making the assumption that all free electrons are concentrated in an infinitely thin layer at a fixed height of 400 km above the Earth's surface.

VTEC variability on days 05 and 06 December 2006 was analyzed focusing on the daytime variations from 06:00 to 18:00 UTC (Coordinated Universal Time). For estimation of VTEC, the closest GNSS stations to the ionosonde stations were selected (Table 2). GNSS stations belong to the EUREF Permanent Network (EPN) and were obtained from: <ftp://epncb.eu/pub>. For the analysis of VTEC variations on 05 and 06 December 2006, the reference VTEC ($VTEC_{quiet}$) was calculated as mean VTEC for quiet days (max X-ray radiation (1–8 Å) $< 5 \times 10^{-6}$)

$$VTEC_{quiet} = \frac{\sum_{i=1}^j VTEC_{quiet(i)}}{j} \quad (5)$$

where j are the number of VTEC data within the quiet period. The selected quiet period has been selected based on the measurements of the GOES satellites (please see above) and it comprises 16 November 2006 to 27 November 2006, and 28 December 2006 to 09 January 2007. Figure 3 shows the VTEC changes at the different stations between 16 November

2006 and 09 January 2007, therefore during the investigated days (05 and 06 December) and during the quiet reference periods.

The aim was to analyze the VTEC variations during and after the four investigated flare events at different latitudes of GNSS stations used for VTEC estimation (Table 1; Figure 2). $dVTEC$ represents the difference between observed VTEC and $VTEC_{quiet}$ as

$$dVTEC = VTEC_{obs} - VTEC_{quiet} \quad (6)$$

Relative change of VTEC ($\Delta VTEC$) compared to the VTEC during reference quiet days ($VTEC_{quiet}$) is estimated similarly as for the ionosonde data in (Eq. 2) as

$$\Delta VTEC = \frac{VTEC_{obs} - VTEC_{quiet}}{VTEC_{quiet}} \cdot 100\% \quad (7)$$

2.3 DEMETER VLF measurements

DEMETER was a low Earth orbit satellite operating between 2005 and 2012. Among other experiments, it provided almost

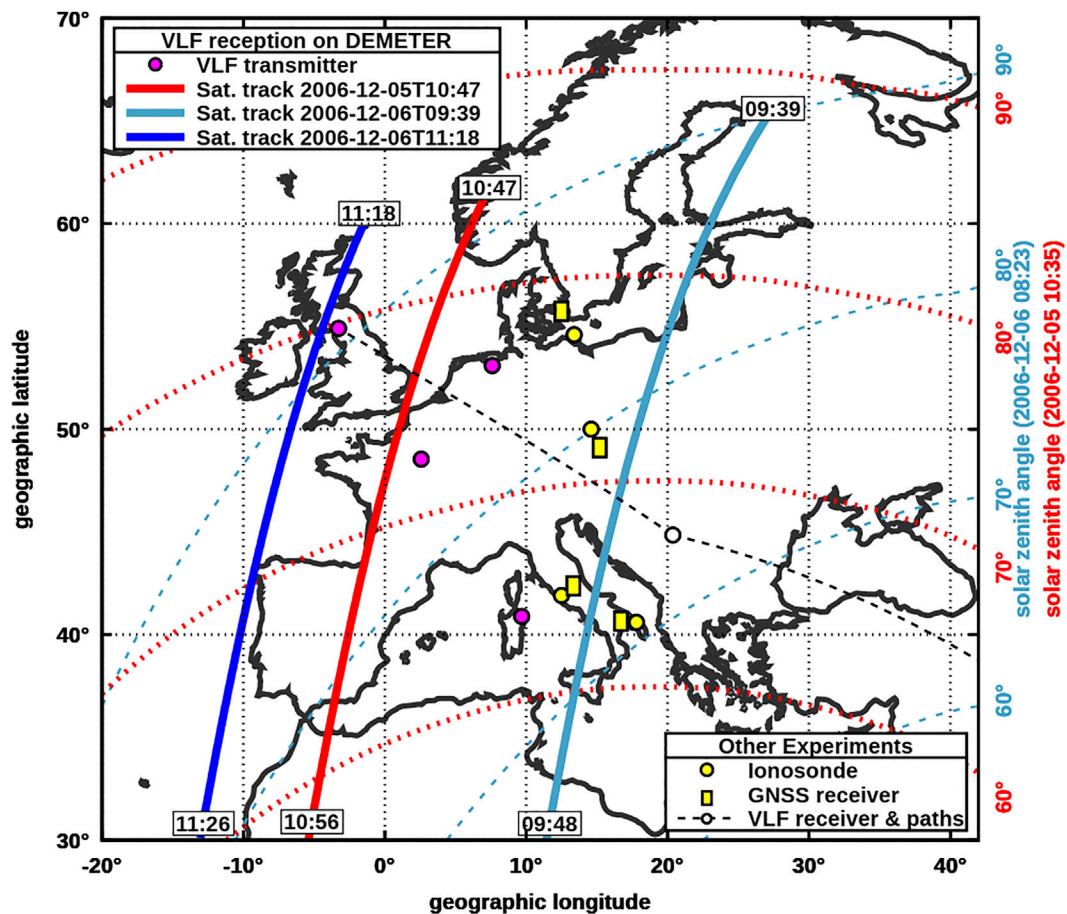


FIGURE 2

Locations of stations/experiments used in this study. The map shows VLF transmitters (magenta dots, north to south: GBZ/GQD in the United Kingdom, DHO in Germany, HWV in France, ICV in Italy) and the ground track of the DEMETER satellite during three separate passes that we used to detect the transmitter signals. Also shown are ionosonde stations (yellow dots, north to south: Juliusruh, Pruhonice, Rome and San Vito), GNSS receivers (yellow squares, north to south: BUDP (Kobenhavn), KUNZ (Kunzak), AQU1 (L'Aquila), MATE (Matera)), and one narrow-band VLF receiver station (white circle, Belgrade) listening to GQD (United Kingdom) and NWC (Australia) transmitters, with the great circle paths between the receiver and the transmitters shown as a black dashed line. In addition, solar zenith angle isolines during two flare events are indicated (X9.0, peak time at 10:35 on 05 December, and M6, peak time at 08:23 UT on 06 December 2006, dashed lines).

continuous coverage of spectral measurements in the VLF band over geomagnetic low and mid-latitudes. For this study, we selected specific half-orbits where the satellite passed during daytime above the VLF transmitters shortly after the candidate solar flare events. Since these measurements are generally restricted to $\pm 65^\circ$ geomagnetic latitudes, we only considered transmitters inside this range.

The satellite includes magnetic and electric field measurements, using its IMSC (Instrument Magnetometre Search Coil) and ICE (Instrument Champ Electrique) instruments, respectively (Parrot et al., 2006; Berthelier et al., 2006), in various frequency ranges and along multiple axes. In this study, we used the survey mode VLF measurements, which provide high resolution spectra extending up to 20 kHz, with a frequency resolution of 19.5 Hz. In survey mode, only one

channel of electric and one channel of magnetic measurements are stored. Despite the Nyquist frequency being 20 kHz, a number of transmitters (DHO, HWV, ICV) emitting slightly above 20 kHz also appear in the records due to frequency aliasing.

While the VLF survey mode stores only one component of both the electric and the magnetic fields, according to Cohen and Inan (2012) Poynting flux can be reasonably estimated from these two components. In the selected time periods we were able to identify the VLF transmitter signals in the electric measurements but not in the magnetic spectra, due to high noise levels. This can still provide an estimate of the Poynting flux (due to low E/cB values, again noted by Cohen and Inan, 2012), but we did not want to introduce more uncertainties. Instead, we compare E-field measurements directly to

TABLE 2 Class, date, peak time of the investigated flares, furthermore the latitude and solar zenith angle at the peak time of the flares of the different ionosonde station, and the detected duration of fade-out (at the time of the flare), df_{min} and Δf_{min} variation (at the time of the flare and/or measured after the fade-out).

Class of flare, date	Peak time (UTC)	Intensity [Wm^{-2}]	Station	Latitude [°]	Zenith angle [°]	Duration of fade out [min]	df_{min} [MHz]	Δf_{min} (%)
M1.8, 05-12-2006	8:03	1.84E-05	Juliusruh	54.6	85.6	0	0	0
	8:03	1.84E-05	Pruhonice	50	81.7	0	0	0
	8:03	1.84E-05	Rome	41.9	76.5	0	1.1	65
	8:03	1.84E-05	San Vito	40.6	73.1	0	0	0
	8:03	1.84E-05	Ascension Isl.	-7.95	70.4	0	1.1	59
	8:03	1.84E-05	Madimbo	-22.38	24.8	30	0	0
	8:03	1.84E-05	Grahamstown	-33.3	29.5	0	1.8	71
X9.0, 05-12-2006	10:35	9.06E-04	Juliusruh	54.6	77.15	0	4.3	285
	10:35	9.06E-04	Pruhonice	50	72.5	30	2.1	105
	10:35	9.06E-04	Rome	41.9	64.64	60	2.1	81
	10:35	9.06E-04	San Vito	40.6	63.05	30	2.4	145
	10:35	9.06E-04	Ascension Isl.	-7.95	36.14	60	4.1	153
	10:35	9.06E-04	Madimbo	-22.38	9.63	90	3.5	79
	10:35	9.06E-04	Grahamstown	-33.3	12.29	75	3.5	79
M6.0, 06-12-2006	8:23	6.08E-05	Juliusruh	54.6	83.21	0	0	17
	8:23	6.08E-05	Pruhonice	50	79	0	0.5	48
	8:23	6.08E-05	Rome	41.9	73.19	15	3.1	133
	8:23	6.08E-05	San Vito	40.6	69.98	0	1.9	117
	8:23	6.08E-05	Ascension Isl.	-7.95	63.51	75	3.2	127
	8:23	6.08E-05	Madimbo	-22.38	18.16	90	4.1	127
	8:23	6.08E-05	Grahamstown	-33.3	23.49	75	3.6	90
C4.8, 06-12-2006	12:58	4.82E-06	Juliusruh	54.6	81.4	0	0	0
	12:58	4.82E-06	Pruhonice	50	77.7	0	0	7
	12:58	4.82E-06	Rome	41.9	70	0	0.5	25
	12:58	4.82E-06	San Vito	40.6	71	0	0	6
	12:58	4.82E-06	Ascension Isl.	-7.95	14.8	0	3.6	135
	12:58	4.82E-06	Madimbo	-22.38	48.5	0	0.3	20
	12:58	4.82E-06	Grahamstown	-33.3	39.8	0	0.7	30

measurements made on reference days, to discern any differences due to different ionospheric conditions.

The reference periods were chosen such that the satellite ground tracks are almost identical (to a few km) to the study periods, and the satellite altitude is also the same (670 km), in order to reduce any differences in reception arising from a different geometry. Due to the Sun-synchronous orbit, local times are also the same, and all reference periods are on geomagnetically quiet days. For each observation we used a set of four such reference passes. Figure 9 shows detected transmitter power during the three selected flare events, and comparison to the corresponding reference periods. To process the broadband spectra, for each transmitter we took the corresponding frequency bin and subtracted the average of the neighbouring frequency bins to remove any wide-band noise. On some days some of the transmitters were not operational, we

confirmed this by looking at ground-based VLF records and excluded those from the reference curves shown on Figure 9.

2.4 Ground-based VLF measurements

Observed phase and amplitude data of VLF radio signal is used to obtain electron density and other plasma parameters and quantities for the lowest edge of the Earth's ionosphere at low and midlatitudes during December 2006. The basis for analyzing disturbances induced by solar flares is the measured phase and amplitude of the NWC/19.80 kHz, radio signal (transmitter at North West Cape, Australia 21.816°S, 114.166°E, radiating 1 MW) and GQD/22.10 kHz radio signal (located in the Skelton, United Kingdom, 54.730 N, 2.880 W), at Belgrade site (44.85°N, 20.38°E), Serbia by AbsPAL system (see Table 1). All

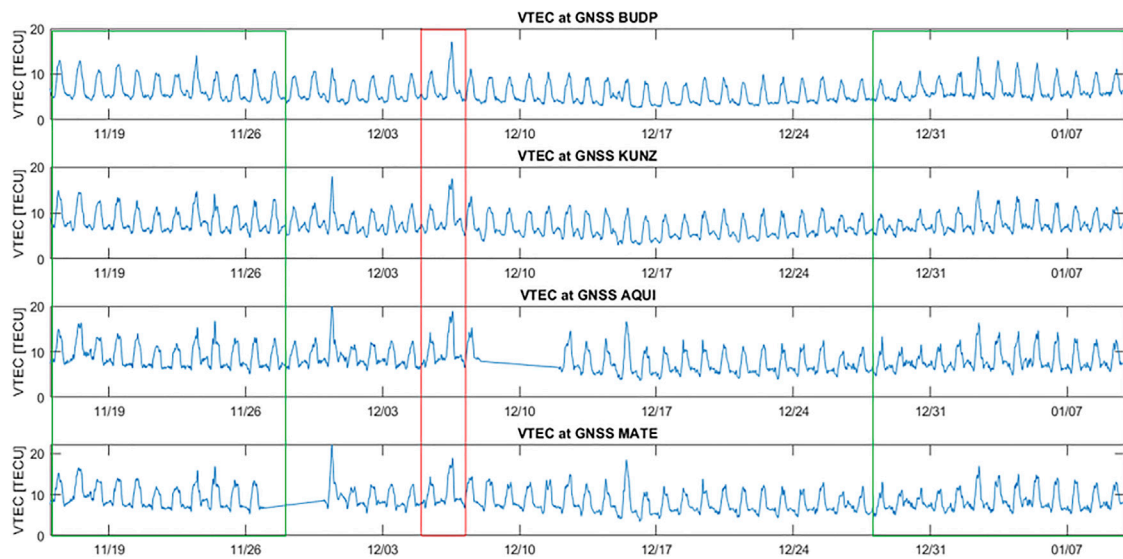


FIGURE 3
VTEC variations for the whole period. Green boxes represent days that are used to estimate the regular VTEC variability (VTEC quiet), while the red box shows the period of the examined solar flares (05 and 06 December 2006).

ground-based VLF data underlying this article will be shared on reasonable request to the corresponding author. The path NWC/19.80 kHz—Belgrade belongs to so called long path (distance between transmitter and receiver $D = 11,980$ km). The path of the VLF radio signal from Skelton to Belgrade is classified as short path ($D = 1980$ km).

For further study we have used Long Wave Propagation Capability, LWPC v2.1 (Available online: <https://github.com/space-physics/LWPC>), a computer program developed by the US Naval Ocean Systems Center, NOSC (Ferguson 1998). We adopt the work of the NOSC group by representing the D-region with a “Wait ionosphere” defined by two quantities, the reflection height, H' , in km, and the “sharpness” of the lower ionospheric boundary β , in km^{-1} (Wait and Spies, 1964). The expression for the electron density in the D-region can be presented by two-parameter analytical formula:

$$N_e(h, H') = 1,43 \cdot 10^{13} \exp(-0,15 \cdot H') \exp[(\beta - 0.15) \cdot (h - H')] \text{m}^{-3} \quad (8)$$

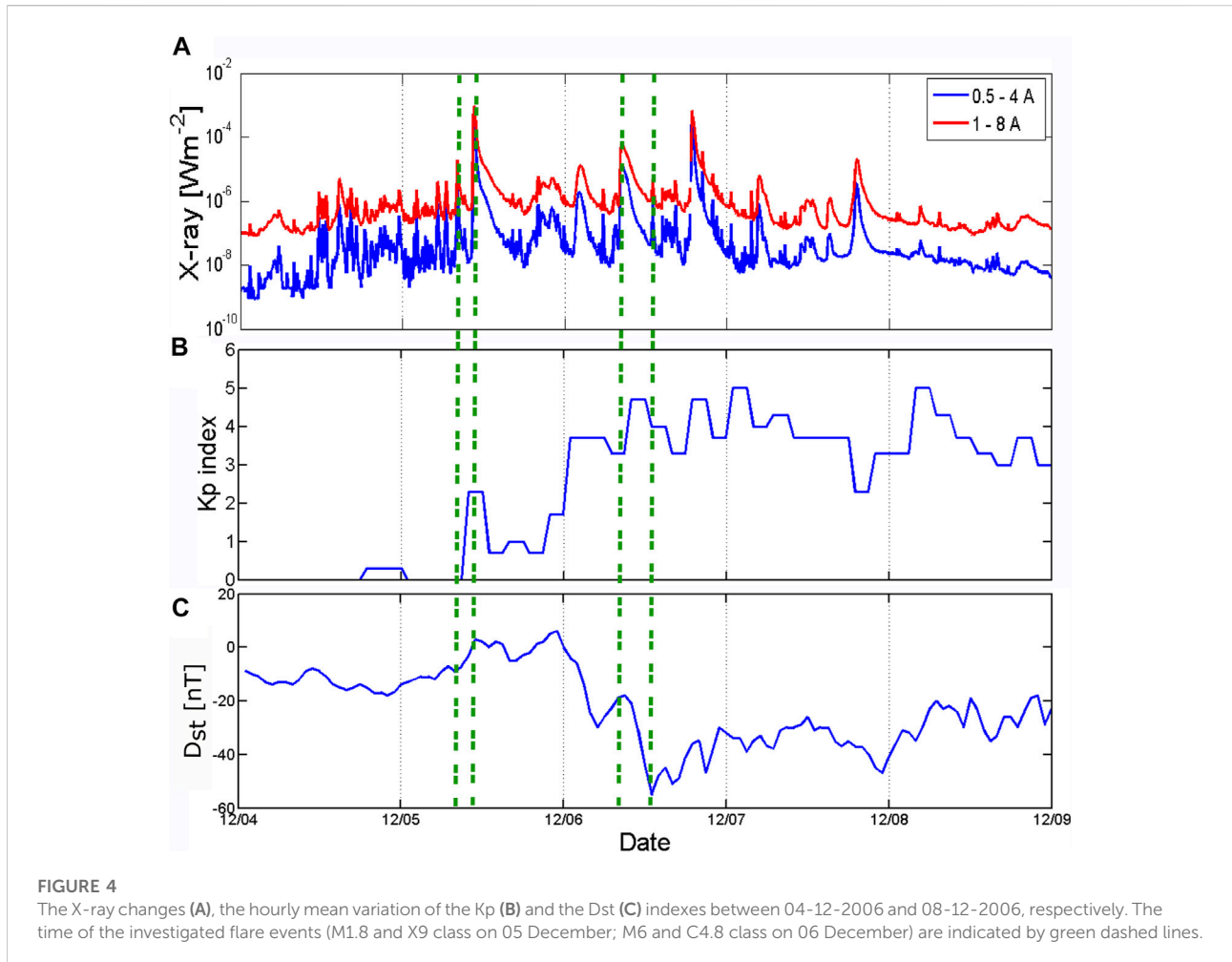
where h is the height in km, β and H' are model parameters, i.e., Wait’s parameters. This model has been used to simulate altitude electron density profile in the D-region at regular conditions, as well as for the perturbed conditions (Šulić et al., 2016). A numerical method for the calculation is based on comparison of the registered changes of amplitude and phase with the corresponding values obtained in simulations using the LWPC numerical software package as explained in e.g., Šulić and Srećković (2014).

3 Results

Four flare events were selected for the investigation which occurred at 08:03 UT (M1.8) and at 10:35 UT (X9.0) on 05 and at 08:23 (M6) and at 12:58 UT (C4.8) on 06 December 2006 (Table 2, upper plot on Figure 4). In this study, we focus on the impact of the flares on the different regions of the ionosphere. Nevertheless, we also took into account variation of Kp and Dst indices (see Figures 4B,C) since they indicate the solar and geomagnetic activity what also affect the state of the ionosphere. The time of the selected flare events are indicated by green dashed lines. As seen on the Kp and Dst variation ($Kp_{\max} = 5$, $Dst_{\min} = -60$, Figures 4B,C) the X9 flare occurring on 05 December 2006 is followed by a minor (G1) geomagnetic storm on 06–08 December 2006. The ionospheric response to the selected flares is detailed in the following subsections.

3.1 Ionosonde data

The advantage of the ionospheric sounding measurements is that the different parameters refer to the changes occurring at the different altitudes/regions of the ionosphere. The foF2 parameter (see Figure 1), the critical frequency, is the maximum plasma frequency of the F2 region. While the fmin parameter (minimum frequency) is sensitive to the variations occurring in the lower ionosphere (D-, E-region). Therefore, investigating more parameters together one can interpret the changes happening at different heights of the ionosphere.



In the first investigation we examined the variation of f_{min} parameters measured at European stations. Data detected at South-African stations have also been analysed in this case for comparison. Figure 5 shows variation of the X-ray flux (upper plots) and of the df_{min} (A) and Δf_{min} parameters (B) detected at different stations (from higher to lower latitudes) on 05 December 2006. The impact of the X9 class flare that occurred at 10:35 on 05 December 2006 (marked by green dashed line) can be clearly seen at every station, even at Juliusruh which is almost a sub-auroral station. Total radio fade-out was detected at mid- and low-latitude stations. Furthermore, enhanced values (2–4.5 MHz) of the df_{min} parameter (the difference of the f_{min} from the reference days) were observed at every station at the time of the flare or after the total radio blackout. We also analyzed the residuals (relative changes in percentage compared to the reference days) of the f_{min} parameter (Figure 5B) at the time of the flares. It varied between 80%–280% at the different stations during and after the X9 class flare event. Based on the Figure 5 the duration of the fade-out, the

enhanced values of the df_{min} and Δf_{min} parameters increased with decreasing latitude.

We investigated the latitude and solar zenith angle dependence of the observed parameters in detail. Table 2 shows the changes of the parameters (duration of the total blackout, df_{min} and Δf_{min} parameters at the different stations) that occurred during the investigated flares. The duration of the total radio fade-out, occurred as a consequence of the X9 flare, clearly shows a solar zenith angle dependence. However, solar zenith angle dependence is not that evident in the cases of the df_{min} and Δf_{min} values. This can be explained by the times of the fade-out being very different at the different ionospheric stations. Therefore, the first parameters just after the fade-out were detected at different times when the X-ray radiation of the flare was also different. E.g., the largest changes of the df_{min} and Δf_{min} parameters were observed at Juliusruh (4.3 MHz and 280% respectively), but no radio blackout was observed there. The reason for the total fade-out and also for the enhanced values of the parameters is the increased absorption of the radio waves in the ionosphere caused by the X9 solar flare.

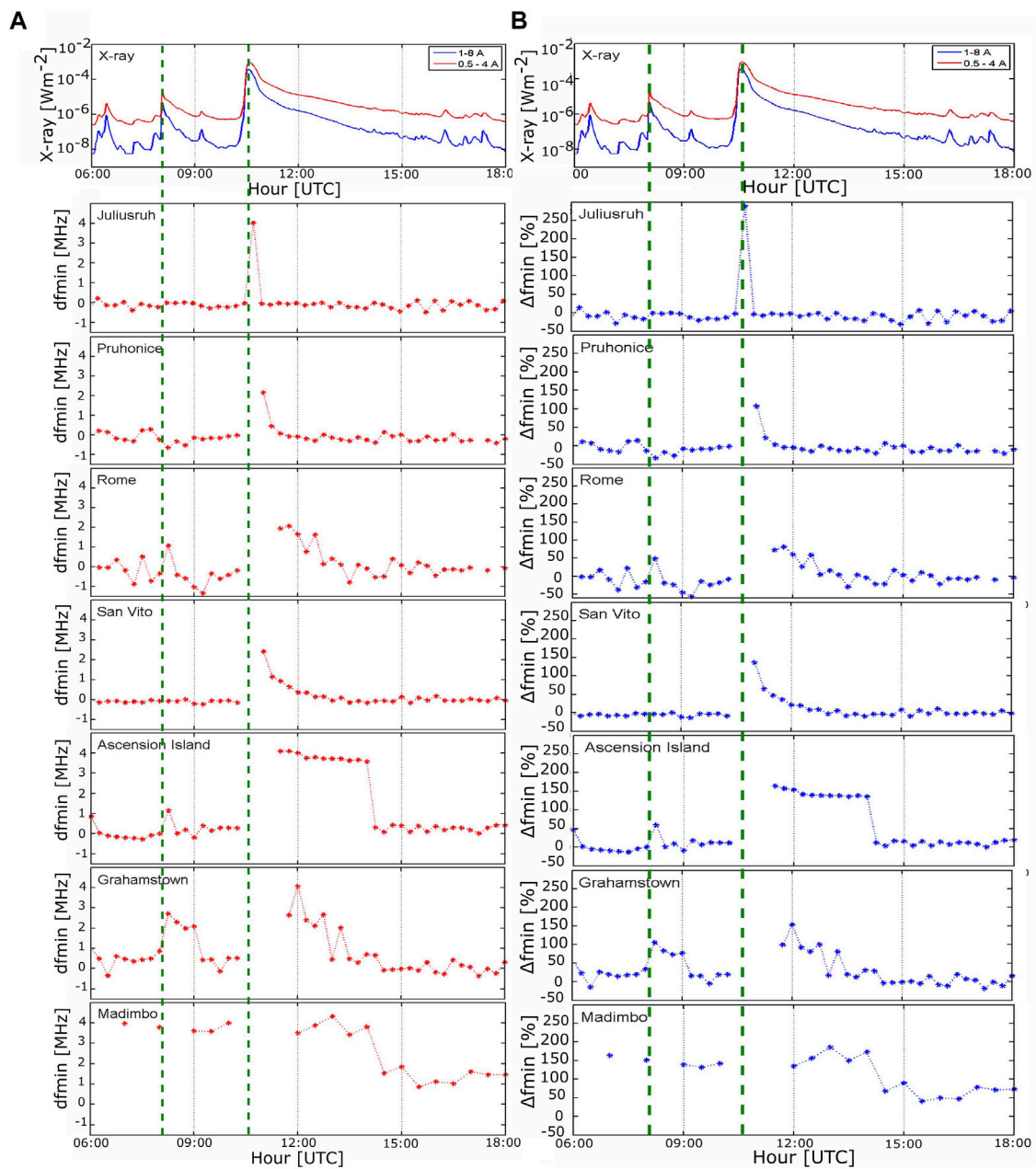


FIGURE 5

The variation of X-ray flux (upper plots) and the df_{min} (A) and Δf_{min} parameters (B) detected at different stations (from higher to lower latitudes) between 06:00 and 18:00 on 05 December. The green dashed lines indicate the time of the investigated flares.

An M1.8 class flare also occurred on 05 December 2006 (peak time at 08:03 UT, marked by green dashed line). However, its impact can be seen only at the South-African stations and at Rome ($df_{\text{min}} \sim 1\text{--}1.5$ MHz, $\Delta f_{\text{min}} \sim 60\%\text{--}70\%$, Figure 5). At Madimbo station (the solar zenith angle was smallest (24.8°) there at the time of the flare) even total radio fade-out was detected during this event. Nonetheless the impact of the flare was undetectable at most of the

European stations under higher solar zenith angle (Juliusruh, Pruhonice, San Vito).

The Figure 6 shows the df_{min} and Δf_{min} variation from 06:00 to 18:00 on 06 December. Analysing df_{min} variation on 06 December the impact of the M6 flare (peak time at 08:23, green dashed line) can be seen at lower latitude European stations (Rome, San Vito) and in South-Africa. At South-African stations even a longer (75–90 min) total radio blackout was detected after

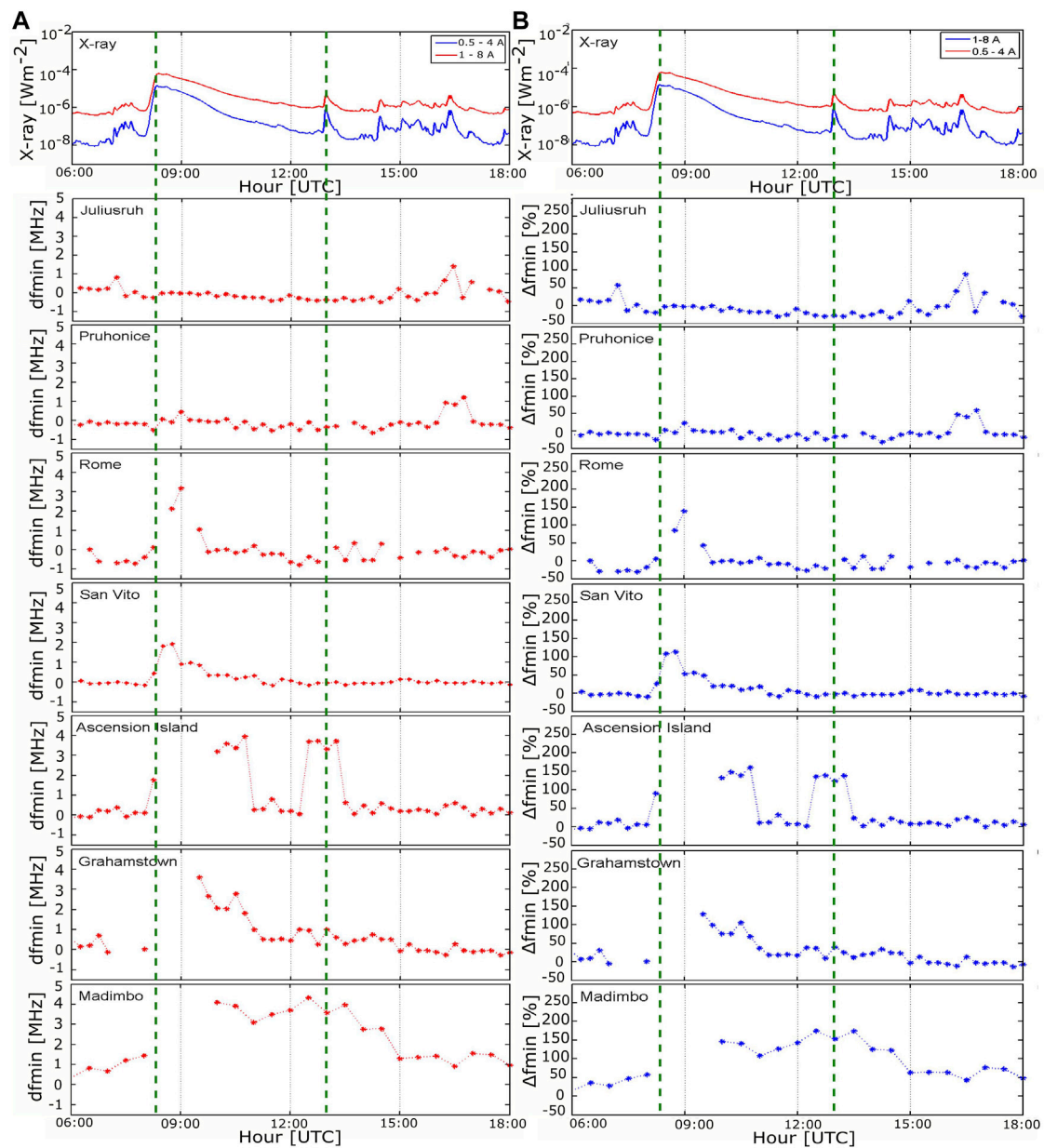


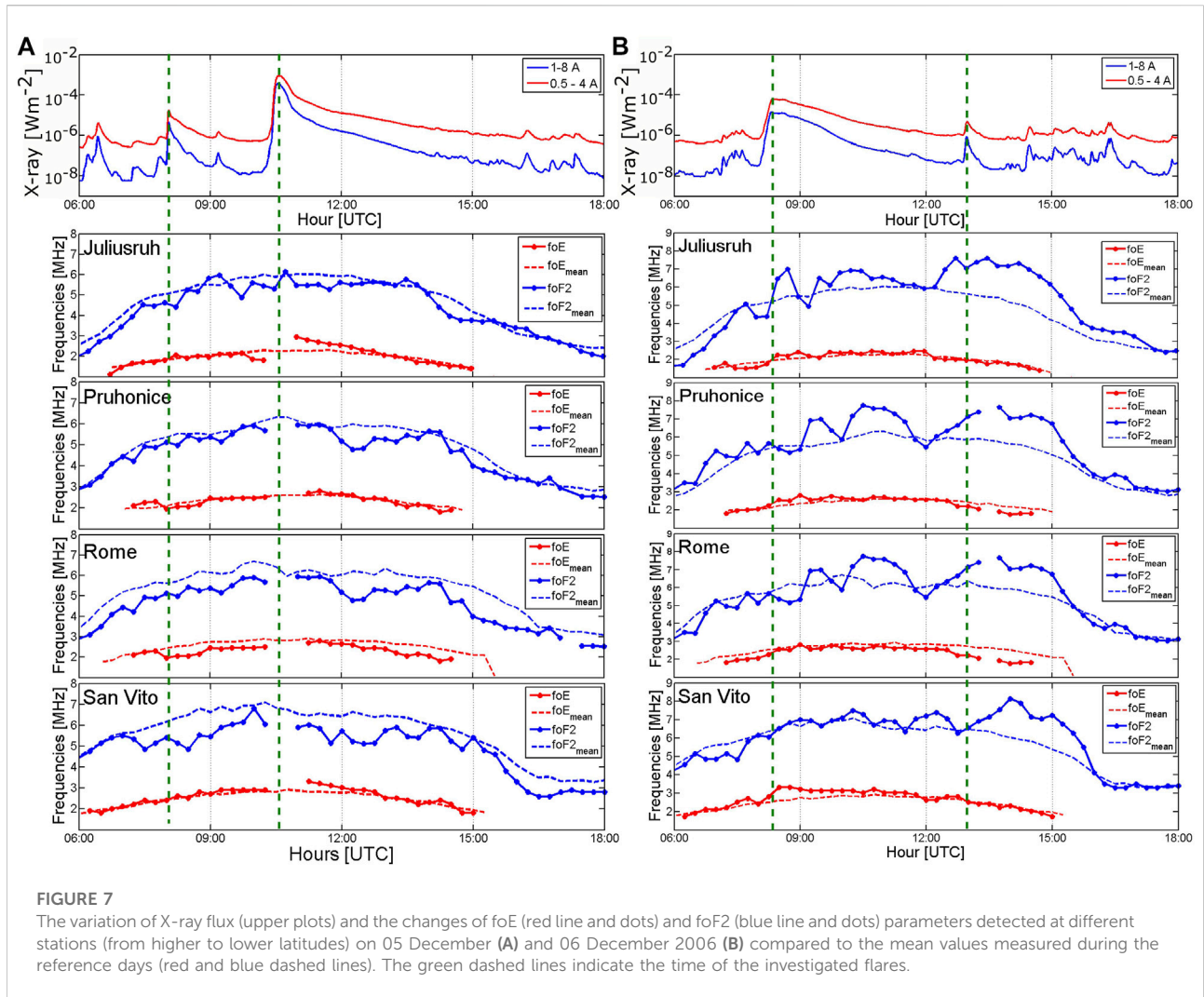
FIGURE 6

The variation of X-ray flux (upper plots) and the df_{min} (A) and Δdf_{min} parameters (B) detected at different stations (from higher to lower latitudes) between 06:00 and 18:00 on 06 December. The green dashed lines indicate the time of the investigated flares.

the M6 flare. Its duration was the longest at Madimbo station which was located under the smallest zenith angle (18°) among the investigated stations. The df_{min} variation varied between 0.5–4 Mhz and it tends to show solar zenith angle dependence (Table 2; Figure 6A). While the observed values of the Δdf_{min} were between 17 % and 133%. The changes of both parameters are larger than in the case of the M1.8 flare (df_{min} : 1–1.8 MHz, Δdf_{min} : 60–70%), that occurred about a day earlier (peak time at 08:03) when the stations had been located under similar zenith

angles. Therefore, the ionospheric response highly depends on the X-ray flux of the flare event, too.

Moreover, the impact of the C4.8 flare (peak time 12:58, green dashed line) was clearly detected only at Ascension Island ($df_{min} \sim 3.6$, $\Delta df_{min} \sim 135\%$) which was under very low solar zenith angle ($\sim 15^\circ$) at the time of the event. Consequently, the strength of the flare event but also the solar zenith angle of the station is very important regarding the impact of the solar events on the ionosphere.



One purpose of this research is to investigate the ionospheric response to the flare events as seen by the different measurement methods. Therefore, we also studied the variation of the foE and foF2 parameters on 05 and 06 December 2006 in order to compare the ionosonde measurements with the VTEC changes based on GNSS observations. The F region with its high electron density provides the largest contribution to TEC (total number of free electrons along the signal's ray path). We concentrated on the changes occurring above the European region in this analysis.

The changes of the foE and foF2 parameters detected at different stations on 05 and 06 December compared to the mean values of the reference days are seen on Figure 7. The total radio fade-out that occurred during the X9 flare on 05 December can be seen in the lack of the foE and foF2 parameters measured at every station (at Juliusruh there is a partial fade-out, the foE parameters are missing while the foF2 increased). However, the impact of the M1.8 flare (peak time at 08:03 on 05 December)

cannot be observed at any parameters detected at the stations. Generally, the foF2 parameters are smaller on 05 December 2006 than the mean values of the reference days, especially at the lower latitude stations (Rome, San Vito), although the difference is relatively small. The effect of the M6 flare (peak time at 08:23 on 06 December 2006, Figure 7B) can be seen in the changes of the foE parameter measured at Pruhonice and San Vito. The foE values are larger directly after the flare onset than the mean values. However, there are no observed similar changes in the foF2 parameter. Furthermore, there are no detectable impacts of the C4.8 flare (peak time at 12:58 UT) on the measured foE and foF2 parameters. A positive ionospheric storm can be seen in the foF2 parameters at every station in the afternoon hours (Figure 7B). It can be caused by the minor geomagnetic storm ($Kp_{max} \sim 5$, $Dst_{min} \sim -50$ nT, Figure 4) that occurred on 06 December 2006. The onset time of the positive ionospheric storm tends to show a latitude dependence. It starts earlier at Juliusruh than at the Italian stations (Rome, San Vito).

We calculated the electron density profiles at the different stations before and after the X9.0 and M6.0 flares (or the total radio fade-outs caused by the flares) by the IRI-2016 model (<http://irimodel.org/>). We used the foE, hmE and foF2, hmF2 values as input parameters for the model from the manually scaled ionograms. We selected observation times after the flare (or after the fade-out) when also the foE parameter was detected in order to compute a more proper electron density profile. Therefore, the observational times before and after the solar flare can differ in the case of the different stations. The results as the output images of the IRI-2016 model and the calculated electron density for the height of the E and maximum of the F region have been summarized in the [Supplementary Material](#). It should be noted that the duration time of the total radio fade-out was the longest at Rome among the European stations, thus the time when also the foE parameter was detected there occurred long after the time of the flare, and thus we do not show the IRI-2016 results for that station. Based on the IRI-2016 model the relative electron density change is 30%–300% in the E region, while it is 5%–30% in the F region as a consequence of the X9.0 flare. Interestingly, the relative electron density change after the M6.0 flare were 5%–60% in the E and also in the F region compare it to the values before the flare. However, the impact of the flare cannot be distinguished from the changes caused by the minor geomagnetic storm in the F region in this case.

3.2 VTEC variations

The $dVTEC$ on 05 December 2006 is shown in [Figure 8A](#). An increase in VTEC values was observed during the solar flare of class X9.0. The peak is especially visible at the GNSS stations in Italy (AQUI and MATE) up to 3 TECU (TEC units) compared to $VTEC_{quiet}$. The increase in ionization was higher over the southern GNSS stations AQUI and MATE than at the northern GNSS stations BUDP and KUNZ. On the other hand, the effect of the less intense solar flare of M1.8 class that occurred in the morning was difficult to observe in $dVTEC$. The second increase of ionization above studied GNSS stations in Italy was observed from around 13:30 UTC, i.e., after the appearance of X9.0 solar flare. This implies the possibility that irregularities in the ionosphere due to increased solar radiation lasted for a longer time.

The relative change ($\Delta VTEC$) during solar flare X9.0 on 05 December 2006 was lowest at the GNSS station BUDP with the highest latitude ([Figure 8C](#)). It can be seen that the $\Delta VTEC$ increased by decreasing the latitude. At the GNSS station KUNZ it reached 10%, while at the southern GNSS stations AQUI and MATE the relative change was more than twice as high (>20%) than VTEC from the GNSS station KUNZ. On the other hand, it was difficult to observe a clear peak in VTEC data that could be

associated with a weaker solar flare of class M that occurred in the morning.

On 06 December 2006, increased ionization was visible during the whole daytime period. Since there was a geomagnetic storm, it increased the VTEC, which is usually referred to as positive storm effects. The M6 and C4.8 solar flares occurred during the initial and the main phase of the geomagnetic storm, respectively ([Figure 4](#)). Therefore, the impact of solar flares on the ionospheric VTEC cannot be investigated for 06 December 2006, as the geomagnetic storm caused the increased ionization in the F layer during the solar flares occurrence. The differences between observed VTEC and $VTEC_{quiet}$ were similar for all four GNSS stations ranging from about 5 TECU to close to 10 TECU ([Figure 8B](#)). VTEC started to increase rapidly after the initial storm phase, reaching the highest ionization after the main geomagnetic storm phase ([Figure 4](#)). VTEC peaks first occurred in the high latitude ionosphere over the GNSS station BUDP. Afterwards, they were recorded in the middle latitude, i.e., by about half an hour to 1 hour later at the southern GNSS stations in Italy ([Figure 8B](#)).

The $\Delta VTEC$ on 06 December 2006 was around 50% to a maximum of 100% at all stations and slightly even higher at the stations in Italy ([Figure 8D](#)). When analyzing the time of VTEC increments and peaks, a time shift from northern GNSS station BUDP (high latitude) to southern GNSS stations AQUI and MATE is visible. That implies that VTEC irregularities from the geomagnetic storm were propagating from high to middle latitudes, and therefore occurred later in the lower latitudes. The amplitude of these perturbations is much higher than the ionization that could be generated by solar flare events. Therefore, this makes it difficult to observe effects from solar flares on the ionospheric VTEC during a geomagnetic storm event and to separate solar flares effects from the ionospheric irregularities produced by a geomagnetic storm.

Colormap of VTEC values during 05 and 06 December are seen on [Figures 8E,F](#). The colors (from blue to red) indicate the VTEC change measured at the different stations. The highest VTEC values on 05 December 2006 were during the X9.0 solar flare, especially for the GNSS stations KUNZ, AQUI and MATE, amounting to about 15 TECU ([Figure 8E](#)). For the southern stations VTEC diurnal values were slightly higher than for the northern stations. On 06 December 2006, VTEC increase was visible with longer duration ([Figure 8F](#)). The larger impact was on the southern stations (AQUI and MATE), i.e., with the higher VTEC values and longer duration of VTEC anomalies, than for the northern station BUDP. Daily VTEC values were affected by the geomagnetic storm from early morning (08:00) to afternoon (16:00). The VTEC peak was visible in the afternoon at around 14:00. Since the VTEC disturbances due to the geomagnetic storm were strong and dominant, the effects of weaker solar flares (M and C classes) could not be detected on 06 December.

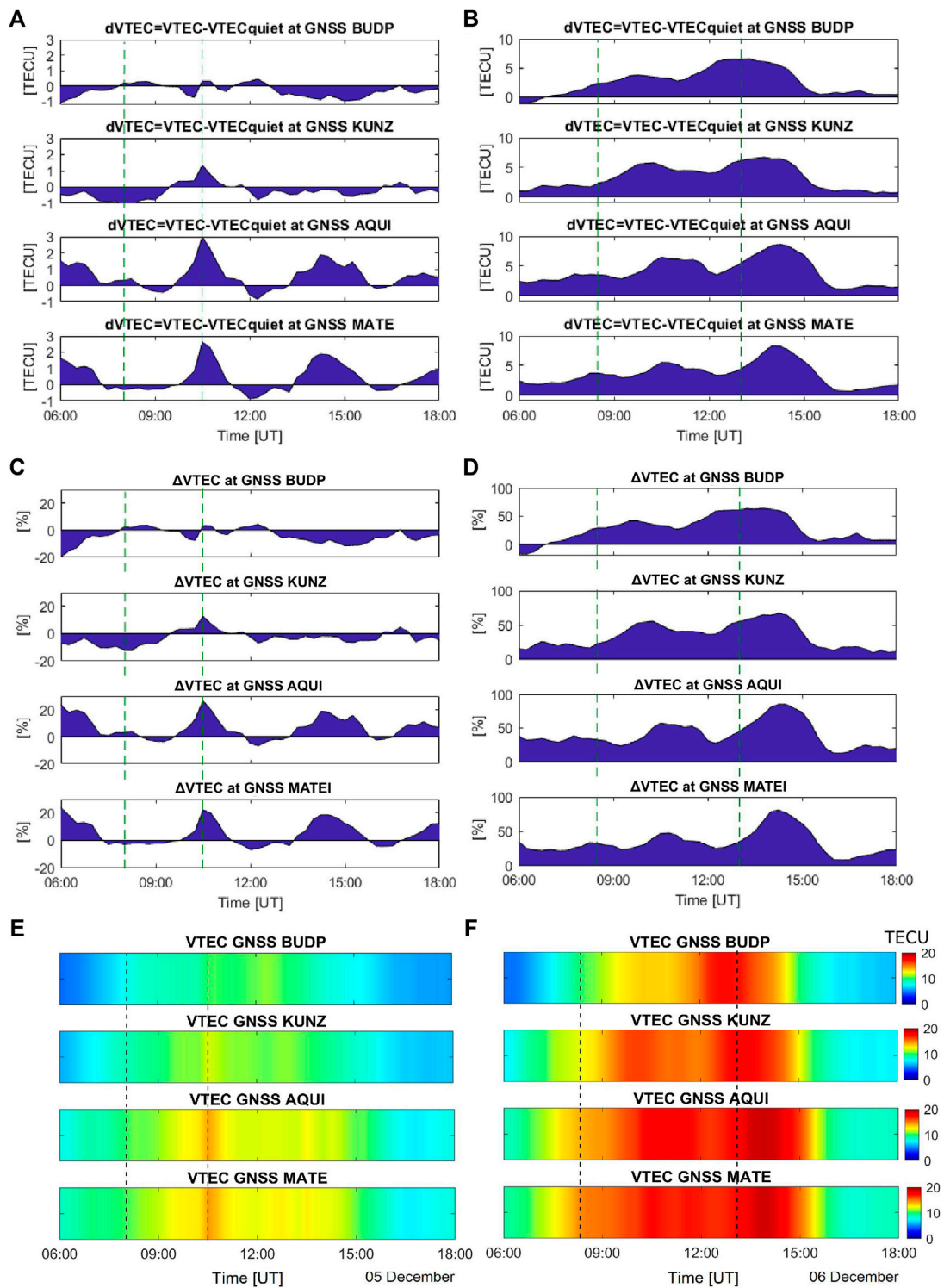


FIGURE 8

05 December 2006: The dVTEC (A) and ΔVTEC (C) on 05 December. Green dashed lines represent the peaks of solar flares, i.e., 08:03 UTC (M1.8) and 10:35 UTC (X9.0). The dVTEC (B) and ΔVTEC (D) on 06 December. Green dashed lines represent the peak of solar flares, i.e., 08:23 UTC (M6) and 12:58 UTC (C4.8). Colormap of VTEC values measured at the different stations during 05 December (E) and 06 December 2006 (F). Black dotted lines represent the peak of solar flares: 08:03 UTC (M1.8) and 10:35 UTC (X9.0) on 05 December, 08:23 UTC (M6) and 12:58 UTC (C4.8) on 06 December 2006.

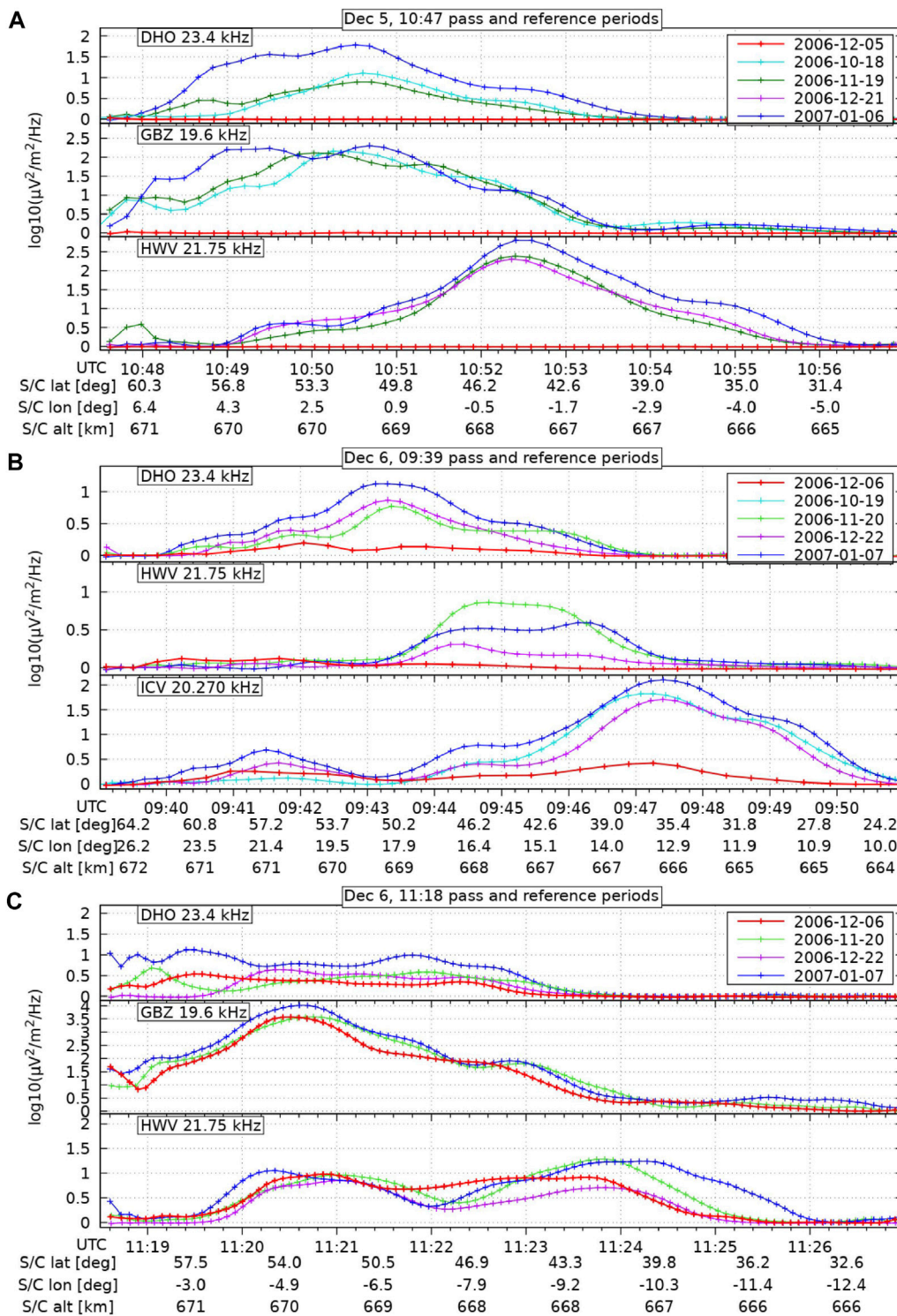


FIGURE 9

Transmitter signal power measured on the DEMETER satellite, during three passes (red curves) and during corresponding reference periods. After the class X9 flare event (05 December 2006, **A**), complete VLF fade-out can be observed (signal falls to background level). About 70 min after the class M flare event (**B**), significant VLF attenuation can be observed. Another 100 min later, no clear difference compared to reference days (**C**).

3.3 Transionospheric VLF absorption (DEMETER data)

We present the observation of ground transmitter signals extracted from broadband spectra of the DEMETER satellite. Figure 9 shows the results during three paths after two selected flare events. The first record starts about 15 minutes after the X9 flare event (05 December 2006, Figure 9A). Total VLF fade-out is observed, all signals are attenuated to background levels. The broadband spectrogram (not shown here) also lacks any VLF sferics during this period, which are otherwise typically present. The second record starts 70 min after an M6 flare event (06 December 2006, Figure 9B). The transmitter signals appear to be attenuated by about 10 dB. Another 100 min later (Figure 9C), the satellite passes above Europe again (although its track is offset to the west, see Figure 2). This time, about 3 h after the flare peak, no significant difference compared to the reference days can be identified. Note that each of the three tracks correspond to a different minimal distance between the satellite and the transmitter, and each transmitter is operated at different power, thus, peak values of the reference curves can be different on each plot in Figure 9. Secondary peaks are due to interference patterns, see Cohen and Inan (2012).

3.4 Ground-based VLF measurements

The measured variations of amplitude and phase on NWC/19.80 kHz and GQD/22.10 kHz radio signals caused by increased X-ray radiation were analyzed during 05 and 06 December 2006. The monitored amplitude and phase changes on the radio signal are a result of increased electron density and lowered reflection height. Ionospheric incubation times and duration of perturbations on VLF radio signals are related to the intensity of the X-ray flare.

The changes of amplitude and phase on NWC/19.80 kHz radio signal against UT monitored at Belgrade site during normal ionospheric conditions (03 and 04 December 2006) together with perturbed 05 and 06 December 2006 are presented on Figures 10A,B. The upper panel of Figures 10A,B show the solar X-ray radiation against universal time on 05 and 06 December 2006 respectively as monitored by the GOES-15 satellite. The solar flares, of classes M1.8 (peak at 08:02 UT) and X9 (peak at 10:35 UT) occurred on 05 December 2006 and M6 occurred on 06 December 2006 (peak at 08:23 UT), as shown. The effects of those flares were observed in sudden changes in phase and amplitude of NWC/19.80 kHz radio signals. The variations in the phase (middle panel) and amplitude (lower panel) of NWC/19.80 kHz radio signal along with the respective X-ray flux during three flares are shown in Figures 10A,B. During events of solar flares of class M1.8 and X9, the whole long path NWC-BEL ($D = 11,980$ km) was illuminated under different solar zenith angles.

The intensities of VLF radio waves change during an SID in ways that depend on several things, e.g., on the frequency, on the angle of reflection, etc. During disturbances in the mid-latitude D-region are most noticeable as changes in phase of VLF radio waves reflected vertically from the top of the waveguide. In quiet times the phase varies smoothly and regularly throughout the day and night region (Ratcliffe, 1972). For details see, e.g., Sulic et al. (2016).

Very high changes of X-ray intensity induced large additional production of electrons in the D-region. The evidence of these SID's is measurable with the increase of phase and amplitude compared to normal daytime levels. For example, sudden ionospheric disturbances caused changes of the VLF amplitude values of $\Delta A \sim 10$ dB and phase of $\Delta\phi \sim 400^\circ$ at the time of maximum X-ray intensity. All these amplitude and phase changes are caused by additional electron density in the D region.

For studying SID VLF signatures on GQD/22.10 kHz we have selected two solar flare events whose occurrences were in time intervals of a few hours around local noon at Belgrade on 06 December 2006 presented on Figure 10C. During these two events of solar flares: M6 (peak at 08:23 UT) and C4.8 (peak at 12:58 UT) classes perturbations on GQD/22.10 kHz radio signal developed with amplitude decrease and phase increase, simultaneously. The intensities of VLF radio signals change during a SID event in ways that depend on the frequency and on the angle of reflection (Ratcliffe, 1972). For example, during the event of the M6 class solar flare the radio signal of frequency NWC/19.80 kHz reflected from the reflection height H' has increased in strength, while the radio signal of frequency GQD/22.10 kHz has decreased in strength. On both VLF radio signals reflected in the D-region, the clearly marked effect of a SID is a sudden change of phase.

For SIDs, a standard procedure for getting ionospheric parameters is based on comparing the registered amplitude and phase variations with the corresponding values computed by the LWPC code, as explained in Sulic et al. (2016). Ne can be obtained from the measured amplitude and phase changes by a trial-and-error method where density profile is modified until the LWPC computed amplitude and phase match with monitored data (Srećković et al., 2021). Thus, the obtained parameters β and H' can be applied for further calculation and simulations (Eq. 8, etc.).

In details, by applying the LWPC code, the propagation of VLF signal was simulated for normal ionospheric condition, with the aim to estimate the best fitting pairs of Wait's parameters, i.e., β_{nor} and H'_{nor} to get values of VLF amplitude and phase as close as possible to the recorded data for a selected day. Next we simulated propagation of VLF signal through the waveguide under the disturbed ionospheric condition. For that we need observed VLF data to examine the signal perturbations during the solar X-ray flare. The selected pair of β and H' is used as input parameter in the LWPC code to obtain the VLF signals

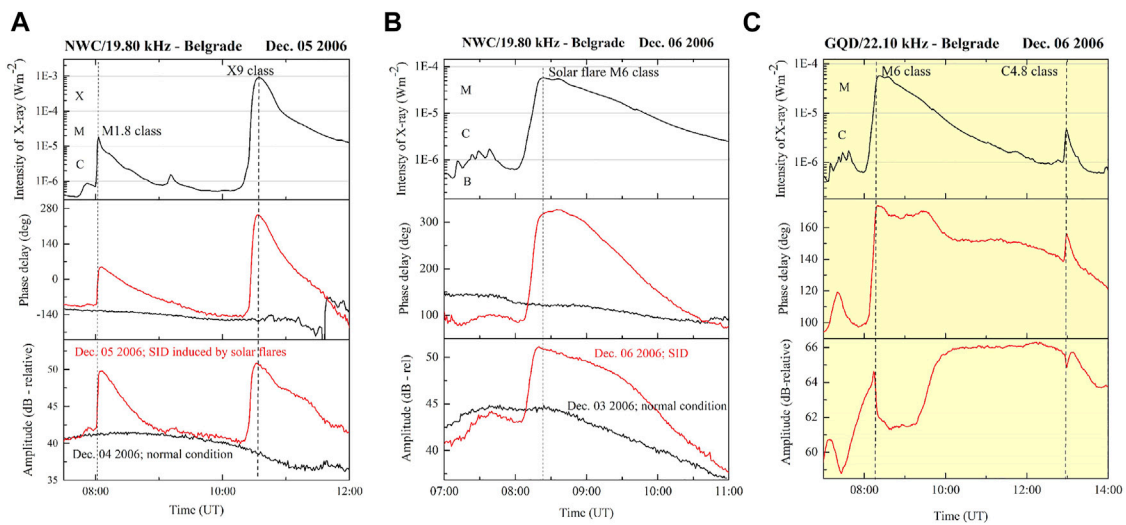


FIGURE 10 Variation of X-ray irradiance (panel 1), phase (panel 2) and amplitude (panel 3) on NWC/19.80 kHz radio signal recorded at Belgrade against UT on normal day, 03 and 04 and disturbed days, 05 and 06 December 2006, respectively. (C) Variation of X-ray irradiance (panel 1), phase (panel 2) and amplitude (panel 3) on GQD/22.10 kHz data recorded at Belgrade against UT on disturbed day 06 December 2006.

i.e., simulated data of amplitude and phase at the receiver site. The process was rerun until differences between the simulated signal ΔA_{sim} and $\Delta\phi_{sim}$ (for the disturbed and normal condition) matched the measured ones ΔA and $\Delta\phi$. After accomplishing a fair matching: $\Delta A_{sim} \approx \Delta A$ and $\Delta\phi_{sim} \approx \Delta\phi$, the corresponding pair of β_{per} and H'_{per} was obtained. In the above expressions the index “sim” means simulated, “per” denote perturbed condition. The obtained pair of β_{per} and H'_{per} was used for calculation of the electron density as a function of height for normal and four solar flare conditions. The obtained parameters β_{per} and H'_{per} can be applied for further calculation and simulations (Eq. 8).

In Figure 11 we present calculated altitude profiles of electron densities under different solar activities, i.e., for different classes of solar flares that occurred on 05 and 06 December 2006.

The first line (black) represents the altitude profile of the electron density under normal ionospheric condition, the red line represents the profile of the electron density induced by the M1.8 solar flare with peak at 08:03 UT ($\beta = 0,42 \text{ km}^{-1}$; $H' = 67 \text{ km}$), blue line shows the electron density versus altitude during the extremely large solar flare X9 with a peak at 10:35 UT ($\beta = 0,54 \text{ km}^{-1}$; $H' = 58,8 \text{ km}$), etc. From this figure we can see that the electron density profiles change with different slopes for different classes of solar flares (from X to C) i.e. different solar activity drastically changes the ionosphere composition of the electron density (few orders of magnitude).

The modelling of VLF propagation in the waveguide under normal ionospheric condition and during four SIDs were done and data are presented in Table 3. Table 3 contains measured values ΔA , $\Delta\phi$, together with calculated values of Wait’s

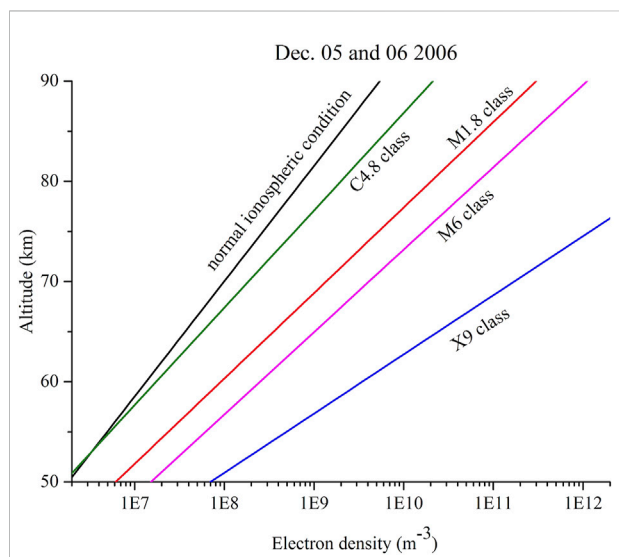
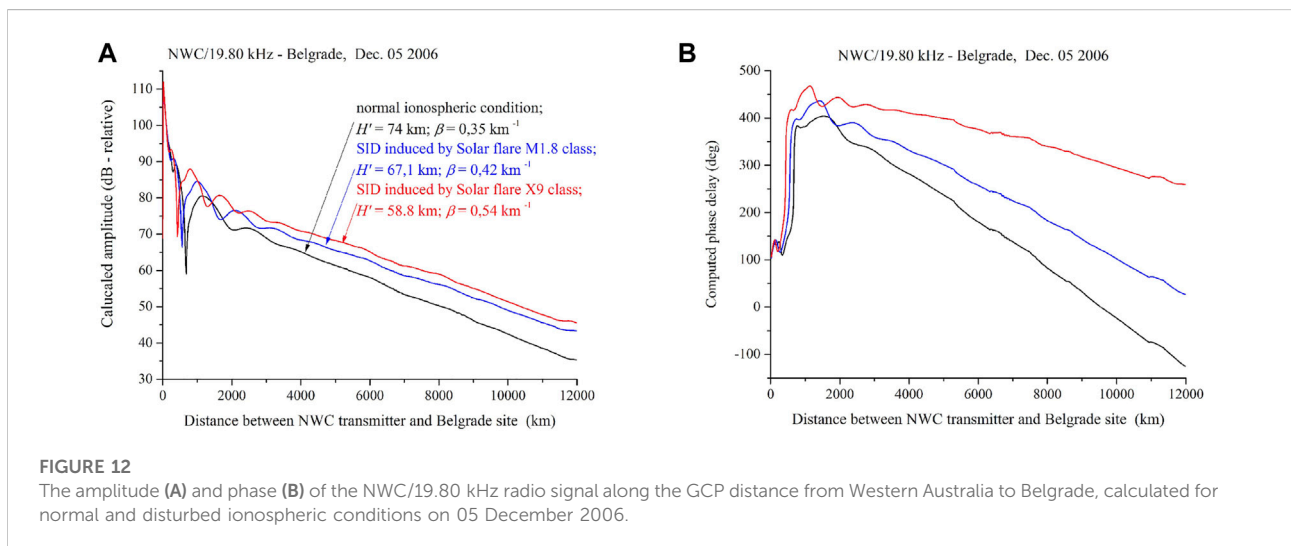


FIGURE 11 Altitude profile of electron density at normal ionospheric condition (black line) and for the four solar flare events occurred on 05 and 06 December 2006.

parameters (quantities obtained by the LWPC code) and electron densities at reflection heights. During a SID, the D-region becomes additionally ionized, the altitude profile of ionospheric conductivity changes and VLF radio signal reflects from a lower height. All of these changes result in different VLF signal propagation compared to the normal ionospheric condition.

TABLE 3 SID VLF signatures and calculated data by LWPC code as a function of intensity of X-ray flux.

NWC/19.80 kHz—BEL path (D = 11,980 km)							
Date	Time UT	Flare class	SID VLF signatures		Calculated data by LWPC code		
			ΔA (dB)	$\Delta\phi$ (deg)	β (km ⁻¹)	H' (km)	$Ne(H')$ (m ⁻³)
05 December 2006	07:00	Normal level	0	0	0.35	74.0	2.16E+08
05 December 2006	08:02	M1.8	7.25	155	0.42	67.1	6.05E+08
05 December 2006	10:35	X9	10.06	415	0.54	58.8	2.33E+09
06 December 2006	08:23	M6	8.03	223	0.43	64.6	1.01E+09
GQD/22.10 kHz—BEL path (D = 1,980 km)							
06 December 2006	12:58	C4.8	-0.7	14	0.389	72	2.98E+08



The increase in the X-ray intensity during the analyzed solar flares changed propagation characteristics of the waveguide with higher values of sharpness and lowering reflection height. For example, additional electron density produced during solar flare X9 class moved the reflection height from 74 to ~59 km and effectively shortened path.

With well-defined β and H' and using the range exponential model of LWPC code it is possible to simulate the amplitude and phase of NWC/19.80 kHz along the propagation path during normal and disturbed ionospheric conditions. Figures 12A,B show simulated amplitude and phase values along GCP distance from transmitter to receiver for normal (at 07:30 UT black lines) and disturbed (at 08:02 UT blue lines and 10:35 UT red lines) ionospheric conditions, i.e., at moments which correspond to maximum X-ray intensity during M1.8 and X9 class flares on 05 December 2006, respectively.

Amplitude values of NWC/19.80 kHz radio signal proportionally grow with increasing X-ray intensity along the whole path. For quiet conditions the phase varies smoothly and regularly throughout the day and night. During the initial and main phase of the SID event the variations are irregular. SID events in the middle latitude D region are mostly noticeable as changes in the phase of VLF radio signals reflected vertically from the region.

4 Discussion

The main purpose of this study is to investigate the ionospheric response to the flare events in the sunlit hemisphere above Europe as seen by the measurements of different instruments. The different techniques used in this research are sensitive to the changes occurring at different

heights, thus regions of the ionosphere. One advantage of ionosondes is that the different parameters obtained from ionograms refer to variations of different ionospheric layers. The minimum frequency (f_{min} parameter) is the rough measure of the HF radio waves absorption in the lower ionosphere (D-, E-region). While the f_oE and f_oF2 parameters are attributed to the maximum plasma frequency (thus the maximum electron density) of the E and F regions respectively. In the case of the Total Electron Content, it is the F region that has the largest contribution to the TEC (Tsurutani et al., 2005). Therefore, the observed VTEC values are sensitive to the ionisation changes mainly occurring in the F region. Based on the DEMETER VLF data, we can obtain information about the absorption of the EM waves in the ionosphere between the transmitter at the ground and the height of the satellite (670 km). Finally, concerning subionospheric VLF signals, the phase and amplitude of the VLF radio signal, propagating in the Earth-ionosphere waveguide between the transmitter and receiver antennas are used to verify electron density parameters for the D-region of the ionosphere. Consequently, investigating the parameters together, we can get a more complete picture of the processes taking place in the whole ionosphere at the time of the solar flares occurred at 08:03 UT (M1.8) and 10:35 UT (X9.0) on 05 and at 08:23 UT (M6) and 12:58 UT (C4.8) on 06 December 2006. This type of comprehensive study is rare in the literature. Generally, studies investigate the ionospheric changes from the perspective of only one observational technique, thus, they are not able to disclose the overall response of the ionosphere to solar flares.

Total radio fade-out was detected at every mid- and low-latitude station during and after the X9-class and M6-class flares on 05 and 06 December (see Figures 5, 6). The duration of the detected total blackout was between 15 and 90 min (Table 2) similar to the findings of previous studies: e.g., Sahai et al. (2007) found lack of echoes on ionograms over the Brazilian sector on 28 October; ~70 min total fade-out was observed after an X2.8 flare (Nogueira et al., 2015) and Sripathi et al. (2013) found a similar phenomenon over the Indian sector during an X7 solar flare on 09 August 2011. Based on detailed analysis of the ionograms, the duration of the total radio blackout seems to show a solar zenith angle dependence. The smaller the zenith angle of the observation site (e.g., at the South-African stations), the longer the observed fade-out of the HF waves.

We also analysed the df_{min} parameter (the difference between the value of the f_{min} and the mean f_{min} for reference days) and the residuals of the f_{min} parameter (Δf_{min} , relative changes in percentage compared to the reference days) during and after the flares. Enhanced values of the df_{min} (0.5–4.5 MHz) and Δf_{min} (17%–280%) were observed during and after the X9 and M6 class flare events (Figures 5, 6). The rate of the increase seems to depend on latitude. However, the solar zenith angle dependence is not that evident as in the case of the duration of the blackout. The reason for that can be that the

fade-out ends at different times, thus the X-ray radiation was different at the time of the detected parameters.

In the case of the less intense solar flares (M1.8 on 05 and C4.8 on 06 December 2006) their impacts were clearly measurable only under small solar zenith angle ($<30^\circ$, see Figures 5, 6). Despite the fact that, the onset time of the M 1.8 flare is almost the same as the M6 flare a day later (08:03 and 08:23 respectively) its impact cannot be seen at the European ionosonde data. It strengthens the main conclusion of Barta et al. (2019), that both the intensity of the flare and the solar zenith angle of the station are very important regarding the impact of the solar events on the lower ionosphere. The reason for the total fade-out and also for the enhanced values of the parameters is the increased absorption of the radio waves in the ionosphere as a consequence of the flare events (e.g., Sripathi et al., 2013; Nogueira et al., 2015; Barta et al., 2019).

We also looked at transionospheric VLF signals measured by the DEMETER satellite. During a satellite pass over Europe 15 min after the X9 class flare event, we observed total VLF fade-out, corresponding to at least 20 dB attenuation (Figure 9A). This is in contrast to the relative minor variations of the transmitter signals between the reference curves, which is less than 10 dB. During a satellite pass 70 min after the M6 class event, significant VLF attenuation could be observed, while the transmitter signals are still clearly present (Figure 9B). In the case of the transmitter that is closest to the satellite ground track, ICV/Isola di Tavolara, the attenuation is about 10 dB. We note that this location experienced the M6-class flare at a higher solar elevation/smaller solar zenith angle ($SZE \approx 75^\circ$) than the other transmitters concerned. Moreover, comparing the signal (red curve) to the records on the reference days we can see that the attenuation is larger at lower latitudes in all the three cases which also indicate a solar zenith angle dependence. Over the next pass, about 80 min later and about 150 min after the M6-class event, the transmitter signals do not exhibit anymore a clearly recognizable deviation from their reference day values (see Figure 9C).

Changes in transionospheric VLF signal levels during the selected solar flare events are consistent with electron enhancements and agree with the results presented in the previous sections. The direct problem of modelling transionospheric VLF attenuation remains a difficult subject, despite recent advances (Graf et al., 2013), with large inaccuracies (on the order of ± 6 dB). In addition, conditions during a solar flare may cause a deviation of attested ionospheric electron density profiles and temperatures, also affecting the wave propagation. An attempt at the inverse problem of estimating electron density changes from the observed attenuation shall require a separate, dedicated investigation.

An increase in VTEC values was observed during the X9.0 class solar flare (Figure 8A). The increase was higher (up to 3 TECU) at lower latitude stations (Italy) than at higher latitudes. Similarly, to the results observed by the ionosondes, the

smaller the latitude (solar zenith angle) the larger the detected f_{min} parameter and the duration of the fade-out. It agrees well with the results of previous studies showing a correlation between the enhanced ionisation in the daylight hemisphere and solar zenith angle (Hernandez-Pajares et al., 2012; Sripathi et al., 2013; Xiong et al., 2014). This hypothesis was also strengthened by the findings of Carrano et al. (2009) who studied the impact of the same X9.0 flare on TEC measured at a low-latitude GPS receiver at Ascension Island. They reported that during this event the TEC increased by approximately 4.3 TECU in 12 min. While the solar zenith angle was quite low, $\sim 33^\circ$ (at 1,045 UT, Carrano et al., 2009). Similar increases were not detected in the foE and foF2 parameters (Figure 7A). However, at the time of the X9 flare there was a total radio fade-out at almost every ionosonde station, except at Juliusruh. There, the foF2 increased from 5.3 to 6.1 MHz at the time of the flare, it means a $\sim 15\%$ variation what is comparable with the 5%–20% changes detected in TEC at the different European stations. The impact of the smaller solar flare (M1.8) that occurred in the morning was difficult to observe in $\Delta VTEC$. A clear effect was observed only under very small solar zenith angles ($<30^\circ$) based on the results of the ionosondes, too.

Investigating the residuals for VTEC and f_{min} parameters (calculated by Eq. 2), the rate of change increased by decreasing the latitude in both cases (see Figures 8C,D). Comparing their values, it varied between 10% and 20% for VTEC, while the Δf_{min} was between 85% and 285% for the same latitude stations in Europe during the X9 flare. The reason for such a difference of the observed percentage can be that the X-rays penetrate to lower heights and ionise the D and E regions while enhancements in the EUV more strongly affect the ionospheric F region. Since different components of the solar irradiance spectrum affect the ionospheric layers differently, we can expect different responses in the lower and higher ionosphere. Consequently, X-ray flares cause higher changes in the ionisation (and also in the absorption) in the D-, E-region than in the F region. Therefore, the f_{min} parameter, which is a good marker of the changes of the lower ionosphere, shows larger changes in percentage, than the VTEC which is sensitive to the changes occurring mainly in the F region (Tsurutani et al., 2005). Mendillo et al. (1974) found 15%–30% TEC increase with larger enhancement at lower latitudes during the great solar flare of 7 August 1972 (estimated class is X20 by Ohshio (1974) using the TEC measurements at 20 locations. Tsurutani et al. (2005) investigated the global ionospheric effects of the X17 flare on 28 October 2003 and found that the VTEC increased to 30% within a few minutes lasting for about 3 h. In contrast, Sharma et al. (2010) found 50%–100% enhancement of the f_{min} parameter during six less intense solar flares occurring in 1999.

The effects of the M6 and C4.8 solar flares on 06 December 2006 cannot be observed in the VTEC variations during a geomagnetic storm of class G1 (Figure 8B). The results reveal a positive ionospheric storm with a whole-day duration. VTEC

increased by up to 5–10 TECU, representing the VTEC change of around 50% to a maximum of 100% at all GNSS stations (Figure 8D). This is much higher than the ionization generated by the solar flare events a day before (10%–20%, see Figure 8C). Prominent positive ionospheric storms with the long-duration were also observed during the stronger geomagnetic storm of class G4, which occurred later on 14 December 2006. The corresponding VTEC enhancement was from 10 to 40 TECU depending on the latitude (Pedatella et al., 2009; Suvorova et al., 2012). It has been suggested that the positive storm effects in the ionosphere are generated from the equatorwards neutral wind, resulting from the high-latitude ionization enhancement (Danilov and Belik, 1992; Pröls. 1995; Kane 2005; Pedatella et al., 2009), as well as from the enhanced eastward electric field (Pedatella et al., 2009). As a result, the F layer height and the electron density in the F layer are increased with long-lasting effects. The magnitude of the storm effects in the ionosphere depends primarily on the latitude, local time, phase, and strength of the storm (Pedatella et al., 2009). Our results show that VTEC values increase firstly in the higher latitude GNSS station BUDP and after 0.5–1 h at the southern GNSS stations in Italy. This can be due to enhanced ionosphere currents through the auroral oval and auroral oval expansion accompanied with the growth of particle precipitation, which led to high-latitude ionization enhancement (Pröls et al., 1991; Danilov and Belik, 1992; Liu et al., 2018). Also, the ionosphere irregularities are considered to be driven by the prompt penetration of electric field during the storm propagating through high latitudes to the middle and low latitudes (Liu et al., 2018), which explains the time delay of detected ionosphere irregularities. The same phenomena was observed in the foF2 changes measured at the European ionosonde stations (Figure 7B). Increased values were detected (2–3 MHz compared to the reference days) at every station during the positive ionospheric storm on 06 December. Also the onset time of the foF2 enhancement tends to show a latitude dependence. In contrast, the foE parameter did not show any changes as a consequence of the moderate geomagnetic storm while the impact of the M6 flare can be clearly seen at Pruhonice and San Vito stations (0.5–0.7 MHz enhancement compared to the reference days, see Figure 7B). Sharma et al. (2010) found that the foE parameter increased ~ 0.5 MHz at Ahmedabad low latitude station during the solar flare on 12 May 1997 which is similar to our detected changes. In terms of electron density of E-region peak it means an increase of $\sim 30\%$ (Sharma et al., 2010). Different layers of the ionosphere react differently to solar flares and geomagnetic storms. The effect of enhanced X-ray and EUV radiation emitted by the flare is more pronounced in the E region as it can be seen in the foE parameter variation. While the dynamical changes related to the geomagnetic storm causing such a large variation in the F layer's electron density that the impact of the M6 flare is negligible compared to that. Mansilla (2011) reported positive ionospheric storm in the European

region due to a moderate geomagnetic storm ($Dst \sim -60$ nT) in 19–21 November 2007. The observed foF2 changes (increased about 50%–70%) were comparable to what we observed in the foF2 and VTEC changes during the geomagnetic storm with similar intensity.

A strong solar flare occurred also in the evening hours (class X6.0, peak time: 18:47 UT) on 06 December, therefore Europe was not in the sunlit hemisphere at that time. The event was followed by a solar radio burst which was at least two to three orders of magnitude stronger than all previously known ones and it caused large degradation in the GPS availability and positioning accuracy (Cerruti et al., 2008). Actually, the high-precision regime of positioning of the different type of satellite navigation systems (GPS, GLONASS, GALILEO) over the sunlit hemisphere was partly paralyzed for more than 10 min during the event (Afraimovich et al., 2007). The malfunctioning for these systems for such a long time can be fatal for entire safety systems and cause high financial losses.

The effect of the investigated solar flares is more pronounced in the ground based VLF data, which is sensitive to the changes occurring in the D region. Modified amplitude and phase on NWC/19.80 kHz and GQD/22.10 kHz radio signal are results of increased electron density and lowered reflection height caused by the X-ray flares (Figure 10). The size of amplitude and phase perturbations on VLF radio signals is in correlation with the intensity of X-ray flux, similarly to the results of Šulić and Srećković (2014) and Feng et al. (2021). At the peak time of the X9 flare the observed changes reached $\Delta A \sim 10$ dB for the VLF amplitude values and $\Delta \varphi \sim 400^\circ$ for the phase (see Figure 10A). The detected disturbances are larger than those observed at Belgrade during an X1.3 flare on 7 September 2017 with the values of about +4 dB and +159° (Kolarski et al., 2022). All these amplitude and phase changes are caused by additional electron density in the D region induced by very high changes of X-ray intensity. During events of solar flares M1.8 and X9 class the whole long path NWC-BEL ($D = 11,980$ km) was illuminated under different solar zenith angles. Therefore, no solar zenith angle dependence can be determined with this path (observation technique).

During the flare events occurred at 08:23 UT (M6) and at 12:58 UT (C4.8) perturbations on GQD/22.10 kHz radio signal were registered with amplitude decrease and phase increase, simultaneously (Figure 10C). Sudden changes of phase caused by SID produced from flares can be clearly seen on both VLF radio signals reflected in the D-region. Consequently, also the impact of the less intense solar flare (C4.8) can be clearly seen on the short path VLF observation [between GQD (Skelton, United Kingdom) and Belgrade thus at mid-latitude, see Figure 2]. In contrast, the impact of the C4.8 flare on the df_{min} parameter cannot be seen in Europe, only at Ascension Island, under very small solar zenith angle ($\sim 15^\circ$). Despite the fact that the f_{min} parameter is a rough measure of the lower ionospheric absorption changes (D-, E-region), the VLF

ground-based measurements is a better technique to investigate the fine changes of the electron density of the D region caused by the less intense solar flares.

Altitude profiles of electron densities for the different investigated solar flares were calculated from VLF measurements (Figure 11). The different classes of solar flares drastically change (few orders of magnitude) the electron density of the ionosphere. It strengthens the results of the ionosonde measurements, that the intensity of the X-ray flux also plays an important role in the ionospheric response. Moreover, the observed changes are much more pronounced in the D region compared to the E and F region. Examining the electron density changes at a given height (e.g. at 70 km) it increased by 100% after the C4.8 flare, while the variation is one order of magnitude after the M class and it even reaches the three orders of magnitude after the X9 class flare. Similar electron density changes were calculated by LWPC code as a function of intensity of X-ray flux (Table 3). It agrees with the results of Srećković et al. (2021) the electron density can increase up to a few orders of magnitude after X-ray flares. In contrast, the observed electron density changes after the M6 flare at the E-layer peak is $\sim 25\%$ – 30% (foE varied from 2 to 2.5–2.7 MHz, see Figure 7B) and there are no detectable changes after the C4.8 flare. Even the residual of the f_{min} parameter, which is a good indicator of the changes in the lower ionosphere, increased 100%–150% after the M6 (Figure 5B) and 85%–285% at different latitudes in Europe after the X9 flare (Figure 6B), respectively. Furthermore, there were detectable changes in the VTEC (primarily affected by the F-region) only after the X9 flare and it is only 10%–20% depending on the latitude (see Figures 8A,C). Although, we could not investigate the ionospheric response to the M6 flare by the foF2 and VTEC parameters because of the presence of the moderate geomagnetic storm.

In a comprehensive analysis Feng et al. (2021) compared TEC and VLF changes during C, M and X class solar flares. Our results agree well with their conclusion that VLF are more sensitive to flares than TEC. The M level flares are the lowest in intensity which can cause considerable TEC changes, while the VLF method can detect most C-class solar flares (Feng et al., 2021). They found that the caused disturbances do not only depend on the flare level, but also on other factors (geographical location and local time) that are also in good agreement with our results. However, also the duration of the flare plays an important role in the TEC response. Based on their results the short flare duration is the reason that the TEC is less sensitive to solar flares than VLF signals. They also investigated the impact of X9 flare (05 December 2006) and they did not detect TEC changes while the VLF signal showed instantaneous enhancement and short flare duration. Different wavelength of the solar radiation (flare) can reach the different height of the ionosphere, EUV cause ionization in the E and F region (e.g., Tsurutani et al., 2005; Manju et al., 2009), while X-rays penetrate more deeply into the

ionosphere reaching the D region and causing enhanced ionization and absorption of the EM waves there (Davies, 1990; Sripathi et al., 2013). Since, the electron density in the D region is generally smaller than in the upper part of the ionosphere the caused additional ionization is quite large compare to the previous ionization to be detectable by the VLF method even in the case of a shorter flare duration. While in the F region, where the Ne is generally larger, the eruption needs longer time to cause detectable (by TEC or by ionosondes) extra ionization (comparing to the “before flare period”), because the caused total ionization depends on the intensity (X-ray flux) but on the duration of the flare, too. This explanation is strengthened by the finding of Feng et al. (2021) that if “the duration of the flare will be longer, the temporal change rate and cumulative variation of TEC will be greater, and the response of TEC to the flare will be stronger.” The height-dependent relative electron density variation ($r\Delta Ne$) is well supported by e.g., the one-dimensional model of Le et al. (2007). Based on their simulation it is especially true during wintertime period (thus in the present investigated case). Nevertheless, our results also suggest that the duration of the flare event can be an important factor, too. The effect of the M6 flare (it took ~ an hour) can be clearly seen on the variation of f_{min} (Figure 6) and foE (Figure 7B) parameters measured by the European ionosondes. While the M1.8 class flare occurred approximately at the same time a day earlier but with shorter duration (~20 min) didn't cause any detectable changes in the ionosonde data (see Figures 5, 7A).

We compared our results with a one-dimensional ionosphere theoretical model developed by Le et al. (2007, see more details of the model in Lei et al., 2004a, b) to investigate the solar flare effects of the ionosphere at middle latitude. They defined the relative increase in Ne, $r\Delta Ne = \Delta Ne/Ne_0$ (Ne_0 denotes the Ne without a flare), and found that the largest $r\Delta Ne$ occurs in the E-region (at an altitude about 115 km) with a factor of more than 3. It strengthens our results, since we found even 280% changes in the f_{min} parameter after the X9.0 flare comparing it to the reference days, what is sensitive for the lower ionosphere. The $r\Delta Ne$ remains below 1 in the F region, especially in wintertime (see Figures 3, 4. in Le et al., 2007), what also agrees with our results of 5%–20% variation in ΔTEC in Europe and $foF2$ parameter measured at Juliusruh during the X9.0 flare. Furthermore, we calculated the electron density profiles at the different stations before and after the large flares (or fade-outs) by the IRI-2016 model based on the parameters derived from the manually scaled ionograms (please see the [Supplementary Material](#)). We selected observation times after the flare (after the fade-out) when also the foE parameter was detected in order to compute a more proper electron density profile. Basically, the IRI-based electron profiles agree well with the one-dimensional ionosphere theoretical model of Le et al. (2007) that the relative variation occurred in the E region is larger than in the F region. The relative electron density change is 30%–300% in the E region,

while 5%–30% in the F region as a consequence of the X9.0 flare. Interestingly, the relative electron density change after the M6.0 flare were 5%–60% in the E and also in the F region compare it to the before flare period. However, we cannot distinguish the impact of the flare from the changes caused by the minor geomagnetic storm in the F region. Moreover, the electron density of the E region ($0.7\text{--}1.2E+11\text{ m}^{-3}$) defined by the IRI-2016 model after the M6 flare for the European region is approximately equal in magnitude to the electron density ($1.2\text{--}1.8E+11$, see Figure 11) at 85–90 km height calculated from the VLF data. Nevertheless, the latter calculation was based on the long and short paths VLF data, thus its result show the ionospheric response also at low latitudes where the expected caused effect is more pronounced than in Europe.

5 Summary and conclusion

In this study we investigated comprehensively the ionospheric response to four solar flares in the European region on 05 and 06 December 2006. The used observational techniques (VTEC, ionosonde data, ground and satellite based VLF method) are sensitive to the changes occurring at different heights, thus regions of the ionosphere. We examined the latitude/solar zenith angle dependence of the observed changes. Furthermore, the intensity of the flare events has also been considered. The main findings of our study are:

- (1) Total and partial radio fade-out were experienced at every ionospheric station during and after the X9 and M6 class solar flares (on 05 and 06 December 2006) and its duration seems to show a solar zenith angle dependence. The smaller the zenith angle of the observation site the longer the detected blackout of the HF waves. The values of the df_{min} (0.5–4.5 MHz) and Δf_{min} (17%–280% compared to the quiet period) parameters measured after the flares/blackouts also increased with the solar altitude during the investigated flares, but they depended on the X-ray flux of the event, too. Nevertheless, the impact of the C4.8 class flare was detectable only at Ascension Island, under a very small solar zenith angle (~15°). The observed changes can be explained by the increased absorption of HF radio waves due to solar flares.
- (2) During a pass over Europe 15 min after the X9 class flare, total VLF fade-out, corresponding to at least 20 dB attenuation, was observed at the DEMETER satellite. During a satellite pass 70 min after the M6 flare, significant VLF attenuation could be observed, and the detected change was the largest in case of the transmitter with a smaller zenith angle than the other sites. Over the next pass, about 150 min after the M6-class event the transmitter signals do not show a clearly recognizable deviation compared to their reference day values.

- (3) During the X9 solar flare we measured a latitude dependent increase of the VTEC values (2–3 TECU). Investigating the residuals for VTEC, the rate of change increased by 10% and 20% with decreasing latitude. On 06 December, the VTEC changes (5–10 TECU) showed increased ionisation (a “positive” ionospheric storm) caused by the minor geomagnetic storm (G1, $Kp_{\max} = 5$, $Dst_{\min} = -60$). VTEC increase due to geomagnetic storm was about three times higher than due to X9 solar flare on the previous day. Consequently, an additional peak in VTEC related to the M6 flare was not observable. Based on our results, the effects of solar flares, even the strong ones, can only be detected in the VTEC data under calm geomagnetic conditions.
- (4) We could not investigate the changes of the foE and foF2 parameters during the X9 solar flare, because of the total radio fade-out at every European ionosonde stations. On 06 December increased foF2 values were detected (2–3 MHz compared to the reference days) at every station during the positive ionospheric storm. However, the impact of the M6 flare was only seen in the foE changes. It increased from 2 to 2.5–2.7 MHz which means a ~25%–30% electron density enhancement at the E-layer peak. While the foE parameter did not show detectable changes after the M1.8 and C4.8 flare.
- (5) Modified amplitude and phase were detected on NWC/19.80 kHz and GQD/22.10 kHz radio signals during every investigated event as a consequence of increased electron density in the D region induced by very high changes of X-ray intensity. The size of the observed perturbations on VLF radio signals was in correlation with the intensity of X-ray flux. Even the impact of the less intense solar flare (C4.8) was clearly seen on the GQD-BEL VLF path, thus at midlatitudes. The different classes of solar flares drastically changed the electron density of the ionospheric D region, as it can be seen in the altitude profiles calculated from the VLF measurements. The electron density around 65–75 km height increased by 100% after the C4.8 class and with one order of magnitude after the M class flares while the rate of change even reached the three orders of magnitude after the X9 class flare. Based on our results the ground-based VLF measurement technique is the most sensitive to the fine electron density changes of the lower ionosphere caused by the less intense solar flares.

Data availability statement

The datasets presented in this study can be found in online repositories. The names of the repository/repositories and accession number(s) can be found below: Global Ionospheric Radio Observatory <http://giro.uml.edu> NASA/GSFC's OMNI data set through OMNIWeb <https://omniweb.gsfc.nasa.gov/> GOES 11 and 12 data, National Oceanic and Atmospheric Administration <https://satdat.ngdc.noaa.gov/sem/goes/data/>

avg/ LWPC v2.1 computer program developed by the US Naval Ocean Systems Center, NOSC <https://github.com/spacephysics/LWPC> GNSS data, EUREF Permanent Network (EPN) <ftp://epncb.eu/pub>. Fortran code for the various versions of the IRI model (International Reference Ionosphere, 2016) used can all be downloaded from <http://irimodel.org>.

Author contributions

VB was responsible for science analysis of the ionosonde data, calculation of the electron density profiles by IRI-2016 model, preparing the initial manuscript and organizing team efforts. RN was responsible for GNSS data processing. VS and DS contributed to the study with the analysis and modelling of the subionospherically propagating VLF signals. KD was responsible for the analysis of the DEMETER data. All members contributed substantially to science discussion and manuscript development.

Funding

The contribution of VB was supported by OTKA, Hungarian Scientific Research Fund (grant no. PD 141967) of the National Research, Development and Innovation Office and by Bolyai Fellowship (GD, no. BO/00461/21). Furthermore, her work was supported by the GINOP-2.3.2-15-2016-00003 project. Author RN acknowledges the German Academic Exchange Service (DAAD) for the Research Grant.

Conflict of interest

The authors declare that the research was conducted in the absence of any commercial or financial relationships that could be construed as a potential conflict of interest.

Publisher's note

All claims expressed in this article are solely those of the authors and do not necessarily represent those of their affiliated organizations, or those of the publisher, the editors and the reviewers. Any product that may be evaluated in this article, or claim that may be made by its manufacturer, is not guaranteed or endorsed by the publisher.

Acknowledgments

Thanks to the International Center of Theoretical Physics (ICTP) Abdus Salam in Trieste and Dr. Luigi Ciruolo for the TEC calibration program, to the EPN network for providing

their GNSS data online for free. Author DK acknowledges the Guest Investigator program issued by CNES providing access to L1 data from the DEMETER mission. The authors are grateful to the University of Massachusetts Lowell Center for Atmospheric Research for the Digisonde data and SAO-X program for data processing. Data from the South African Ionosonde Network are made available through the South African National Space Agency (SANS), who are acknowledged for facilitating and coordinating the continued availability of data. This paper uses data from the Juliusruh Ionosonde, which is owned by the Leibniz-Institute of Atmospheric Physics, Kuehlungsborn. The responsible operations manager is Jens Mielich. This paper uses ionospheric data from the USAF NEXION Digisonde network; the NEXION program manager is Mark Leahy. The authors wish to thank the OMNIWeb

data center for providing web access to the solar data of the Geostationary Operational Environmental Satellites (GOES) satellites. The authors wish to thank the IRI working group for providing the models. The authors appreciate support of the COST Action CA15211, ELECTRONET, in facilitating scientific communication. Thanks to the Institute of Physics Belgrade, through the grant by the MESTD of the Republic of Serbia.

Supplementary material

The Supplementary Material for this article can be found online at: <https://www.frontiersin.org/articles/10.3389/fenvs.2022.904335/full#supplementary-material>

References

- Afraimovich, E. L., Zherebtsov, G. A., and Smolkov, G. Ya. (2007). Total failure of GPS during a solar flare on december 6, 2006. *Dokl. Earth Sc.* 417 (8), 1231–1235. doi:10.1134/s1028334x07080223
- Barta, V., Satori, G., Berényi, K. A., Kis, Á., and Williams, E. (2019). Effects of solar flares on the ionosphere as shown by the dynamics of ionograms recorded in europe and south africa. *Ann. Geophys.* 37 (4), 747–761. doi:10.5194/angeo-37-747-2019
- Berdermann, J., Kriegel, M., Bany 's, D., Heymann, F., Hoque, M. M., Wilken, V., et al. (2018). Ionospheric response to the X9.3 flare on 6 September 2017 and its implication for navigation services over europe. *Space weather.* 16, 1604–1615. doi:10.1029/2018SW001933
- Berényi, K. A., Barta, V., and Kis, Á. (2018). Midlatitude ionospheric F2-layer response to eruptive solar events-caused geomagnetic disturbances over hungary during the maximum of the solar cycle 24: a case study. *Adv. Space Res.* 61 (5), 1230–1243. doi:10.1016/j.asr.2017.12.021
- Berthelier, J. J., Godefroy, M., Leblanc, F., Malingre, M., Menvielle, M., Lagoutte, D., et al. (2006). ICE, the electric field experiment on DEMETER. *Planet. Space Sci.* 54 (5), 456–471. doi:10.1016/j.pss.2005.10.016
- Budden, K. G. (1961). *Radio waves in the ionosphere: The mathematical theory of the reflection of radio waves from stratified ionised layers*. Cambridge, UK: Cambridge University Press.
- Buresova, D., Lastovicka, J., Hejda, P., and Bochnicek, J. (2014). Ionospheric disturbances under low solar activity conditions. *Adv. Space Res.* 54, 185–196. doi:10.1016/j.asr.2014.04.007
- Carrano, C. S., Bridgwood, C. T., and Groves, K. M. (2009). Impacts of the December 2006 solar radio bursts on the performance of GPS. *Radio Sci.* 44, RS0A25. doi:10.1029/2008RS004071
- Cerruti, A. P., Kintner, P. M., Jr., Gary, D. E., Mannucci, A. J., Meyer, R. F., Doherty, P., et al. (2008). Effect of intense december 2006 solar radio bursts on GPS receivers. *Space weather.* 6, S10D07. doi:10.1029/2007SW000375
- Ciraolo, L., Azpilicueta, F., Brunini, C., Meza, A., and Radicella, S. M. (2007). Calibration errors on experimental slant total electron content (TEC) determined with GPS. *J. Geod.* 81 (2), 111–120. doi:10.1007/s00190-006-0093-1
- Cohen, M. B., and Inan, U. S. (2012). Terrestrial VLF transmitter injection into the magnetosphere. *J. Geophys. Res.* 117 (A8). doi:10.1029/2012ja017992
- Danilov, A. D., and Belik, L. D. (1992). Thermospheric composition and the positive phase of an ionospheric storm. *Adv. Space Res.* 12 (10), 257–260. doi:10.1016/0273-1177(92)90475-d
- Davies, K. (1990). *Ionospheric radio*. London Peregrinus.
- Davies, K. (1965). *Ionospheric radio propagation*. Washington DC: Washington U.S. Gov. Print. Off.
- Denardini, C. M., Resende, L. C. A., Moro, J., and Chen, S. S. (2016). Occurrence of the blanketing sporadic E layer during the recovery phase of the October 2003 superstorm. *Earth Planets Space* 68, 80. doi:10.1186/s40623-016-0456-7
- Feng, J., Han, B., Gao, F., Zhang, T., and Zhao, Z. (2021). Analysis of global ionospheric response to solar flares based on total electron content and very low frequency signals. *IEEE Access* 9, 57618–57631. doi:10.1109/access.2021.3072427
- Ferguson, J. A. (1998). *Computer programs for assessment of long-wavelength radio communications, version 2.0: User's guide and source files (No. TD-3030)*. San Diego CA: Space and Naval Warfare Systems Center. Retrieved from <http://www.dtic.mil/docs/citations/ADA350375>.
- K. Folkestad (Editor) (2013). *Ionospheric radio communications* (Kjeller, Norway: Springer).
- Goodman, J. M. (2005). *Space weather & telecommunications*. New York: Springer Science+Business Media, Inc.
- Graf, K. L., Lehtinen, N. G., Spasojevic, M., Cohen, M. B., Marshall, R. A., Inan, U. S., et al. (2013). Analysis of experimentally validated trans-ionospheric attenuation estimates of VLF signals. *J. Geophys. Res. Space Phys.* 118 (5), 2708–2720. doi:10.1002/jgra.50228
- Greninger, P. (2016). *Seasonality of VLF attenuation through the ionosphere*. PhD Thesis. New Mexico: Univ.
- Grubor, D., Sulic, D., and Zigman, V. (2008). Classification of X-ray solar flares regarding their effects on the lower ionosphere electron density profile. *Ann. Geophys.* 26, 1731–1740. doi:10.5194/angeo-26-1731-2008
- Hernández-Pajares, M., García-Rigo, A., Juan, J. M., Sanz, J., Monte, E., Aragón-Ángel, A., et al. (2012). GNSS measurement of EUV photons flux rate during strong and mid solar flares. *Space weather.* 10 (12). doi:10.1029/2012sw000826
- Jiang, H., Wang, Z., An, J., Liu, J., Wang, N., Li, H., et al. (20172017). Influence of spatial gradients on ionospheric mapping using thin layer models. *GPS Solut.* 22 (1), 2. doi:10.1007/s10291-017-0671-0
- Kane, R. P. (2005). Ionospheric fof2 anomalies during some intense geomagnetic storms. *Ann. Geophys.* 23, 2487–2499. doi:10.5194/angeo-23-2487-2005
- Kelley, M. C. (2009). *The earth's ionosphere: Plasma physics and electrodynamics*. Boston: Academic Press.
- Kolarski, A., Srećković, V. A., and Mijić, Z. R. (2022). Response of the Earth's lower ionosphere to solar flares and lightning-induced electron precipitation events by analysis of VLF signals: similarities and differences. *Appl. Sci. (Basel)*. 12 (2), 582. doi:10.3390/app12020582
- Koroncay, D., Lichtenberger, J., Juhász, L., Steinbach, P., and Hospodarsky, G. (2018). VLF transmitters as tools for monitoring the plasmasphere. *J. Geophys. Res. Space Phys.* 123 (11), 9312–9324. doi:10.1029/2018ja025802
- Le, H., Liu, L., Chen, B., Lei, J., Yue, X., Wan, W., et al. (2007). Modeling the responses of the middle latitude ionosphere to solar flares. *J. Atmos. solar-terrestrial Phys.* 69 (13), 1587–1598. doi:10.1016/j.jastp.2007.06.005
- Lei, J., Liu, L., Wan, W., and Zhang, S.-R. (2004b). Model results for the ionospheric lower transition height over mid-latitude. *Ann. Geophys.* 22, 2037–2045. doi:10.5194/angeo-22-2037-2004
- Lei, J., Liu, L., Wan, W., and Zhang, S.-R. (2004a). Modeling the behavior of ionosphere above millstone hill during the september 2127, 1998 storm. *J. Atmos. Solar-Terrestrial Phys.* 66, 1093–1102. doi:10.1016/j.jastp.2004.04.004
- Liu, J. Y., Lin, C. H., Tsai, H. F., and Liou, Y. A. (2004). Ionospheric solar flare effects monitored by the ground-based GPS receivers: theory and observation. *J. Geophys. Res.* 109, A01307. doi:10.1029/2003JA009931

- Liu, Yang, Fu, Lianjie, Wang, Jinling, and Zhang, Chunxi (2018). Studying ionosphere responses to a geomagnetic storm in June 2015 with multi-constellation observations. *Remote Sens. (Basel)*. 10 (5), 666. doi:10.3390/rs10050666
- Manju, G., Pant, T. K., Devasia, C. V., Ravindran, S., and Sridharan, R. (2009). Electrodynamical response of the Indian low-mid latitude ionosphere to the very large solar flare of 28 October 2003—a case study. *Ann. Geophys.* 27 (10), 3853–3860. doi:10.5194/angeo-27-3853-2009
- Mannucci, A. J., Wilson, B. D., Yuan, D. N., Ho, C. H., Lindqwister, U. J., Runge, T. F., et al. (1998). A global mapping technique for GPS-derived ionospheric total electron content measurements. *Radio Sci.* 33 (3), 565–582. doi:10.1029/97RS02707
- Mansilla, G. A. (2011). Moderate geomagnetic storms and their ionospheric effects at middle and low latitudes. *Adv. Space Res.* 48 (3), 478–487. doi:10.1016/j.asr.2011.03.034
- Mendillo, M., Klobuchar, J. A., Fritz, R. B., Da Rosa, A. V., Kersley, L., Yeh, K. C., et al. (1974). Behavior of the ionospheric F-region during the great solar flare of August 7, 1972. *J. Geophys. Res.* 79, 665–672. doi:10.1029/ja079i004p00665
- Mitra, A. P. (1974). *Ionospheric effects of solar flares*. Dordrecht Boston: D. Reidel, Cop.
- Natras, R., Horozovic, D., and Mulic, M. (2019). Strong solar flare detection and its impact on ionospheric layers and on coordinates accuracy in the western Balkans in October 2014. *SN Appl. Sci.* 1, 49. doi:10.1007/s42452-018-0040-9
- Nogueira, P. A. B., Souza, J. R., Abdu, M. A., Paes, R. R., Sousasantos, J., Marques, M. S., et al. (2015). Modeling the equatorial and low-latitude ionospheric response to an intense X class solar flare. *J. Geophys. Res. Space Phys.* 120, 3021–3032. doi:10.1002/2014ja020823
- Ohshio, M. (1974). Solar-terrestrial disturbances of August (1972) Solar x-ray flares and their corresponding sudden ionospheric disturbances. *J. Radio Res. Laboratories Koganei, Tokyo* 21, 311
- Parrot, M., Benoist, D., Berthelier, J. J., Błęcki, J., Chapuis, Y., Colin, F., et al. (2006). The magnetic field experiment IMSC and its data processing onboard DEMETER: Scientific objectives, description and first results. *Planet. Space Sci.* 54 (5), 441–455. doi:10.1016/j.pss.2005.10.015
- Pedatella, N. M., Lei, J., Larson, K. M., and Forbes, J. M. (2009). Observations of the ionospheric response to the 15 December 2006 geomagnetic storm: Long-duration positive storm effect. *J. Geophys. Res.* 114, A12313. doi:10.1029/2009JA014568
- Prölss, G. (2004). *Physics of the earth's space environment: An introduction*. Berlin; New York: Springer.
- Prölss, G. W., Brace, L. H., Mayr, H. G., Carignan, G. R., Killeen, T. L., Klobuchar, J. A., et al. (1991). Ionospheric storm effects at subauroral latitudes: A case study. *J. Geophys. Res.* 96 (A2), 1275–1288. doi:10.1029/90JA02326
- Prölss, G. W. (1995). "Ionospheric F-region storms," in *Handbook of atmospheric electrodynamics*. Editor H. Volland (Boca Raton: CRC Press), 2, 195.
- Ratcliffe, J. A. (1972). *An introduction to the ionosphere and magnetosphere*. Cambridge: The University Press.
- Raulin, J. P., Bertoni, F. C., Gavilán, H. R., Guevara-Day, W., Rodriguez, R., Fernandez, G., et al. (2010). Solar flare detection sensitivity using the south America VLF network (SAVNET). *J. Geophys. Res.* 115 (A7). doi:10.1029/2009ja015154
- Rishbeth, H., and Garriot, O. K. (1969). *Introduction to ionospheric Physics.* NY: Academic Press, 87
- Sahai, Y., Becker-Guedes, F., Fagundes, P. R., Lima, W. L. C., de Abreu, A. J., Guarnieri, F. L., et al. (2007). Unusual ionospheric effects observed during the intense 28 October 2003 solar flare in the Brazilian sector. *Ann. Geophys.* 25, 2497–2502. doi:10.5194/angeo-25-2497-2007
- Schaer, S. (1999). *Mapping and predicting the earth's ionosphere using the global positioning system* PhD thesis. Bern. Switzerland: Bern University.
- Srečković, V. A., Šulić, D. M., Ignjatović, L., and Vujčić, V. (2021). Low ionosphere under influence of strong solar radiation: diagnostics and modeling. *Appl. Sci. (Basel)*. 11 (16), 7194. doi:10.3390/app11167194
- Sripathi, S., Balachandran, N., Veenadhari, B., Singh, R., and Emperumal, K. (2013). Response of the equatorial and low-latitude ionosphere to an intense X-class solar flare (X7/2B) as observed on 09 August 2011. *J. Geophys. Res. Space Phys.* 118, 2648–2659. doi:10.1002/jgra.50267
- Šulić, D. M., and Srečković, V. A. (2014). A comparative study of measured amplitude and phase perturbations of VLF and LF radio signals induced by solar flares. *Serb. Astron. J.* 188, 45–54. doi:10.2298/saj1488045s
- Šulić, D. M., Srečković, V. A., and Mihajlov, A. A. (2016). A study of VLF signals variations associated with the changes of ionization level in the D-region in consequence of solar conditions. *Adv. Space Res.* 57, 4 1029–1043. doi:10.1016/j.asr.2015.12.025
- Suvorova, A. V., Tsai, L. C., and Dmitriev, A. V. (2012). On magnetospheric source for positive ionospheric storms. *Sun Geosph.* 7 (2), 91
- Thomson, Neil R., and Clilverd, Mark A. (2001). Solar flare induced ionospheric D-region enhancements from VLF amplitude observations. *J. Atmos. Sol. Terr. Phys.* 6316, 1729–1737. doi:10.1016/s1364-6826(01)00048-7
- Tsurutani, B. T., Judge, D. L., Guarnieri, F. L., Gangopadhyay, P., Jones, A. R., Nuttall, J., et al. (2005). The October 28, 2003 extreme EUV solar flare and resultant extreme ionospheric effects: comparison to other Halloween events and the Bastille Day event. *Geophys. Res. Lett.* 32, L03S09. doi:10.1029/2004GL021475
- Tsurutani, B. T., Verkhoglyadova, O. P., Mannucci, A. J., Lakhina, G. S., Li, G., Zank, G. P., et al. (2009). A brief review of "solar flare effects" on the ionosphere. *Radio Sci.* 44, 1–14. doi:10.1029/2008rs004029
- Wait, J. R., and Spies, K. P. (1964). *Characteristics of the Earth-ionosphere waveguide for VLF radio waves*, 300. Colorado: NBS Technical Note.
- Xiong, B., Wan, W., Ning, B., Ding, F., Hu, L., Yu, Y., et al. (2014). A statistic study of ionospheric solar flare activity indicator. *Space weather.* 12, 29–40. doi:10.1002/2013SW001000
- Žigman, V., Grubor, D., and Šulić, D. (2007). D-region electron density evaluated from VLF amplitude time delay during X-ray solar flares. *J. Atmos. Sol. Terr. Phys.* 69, 775–792. doi:10.1016/j.jastp.2007.01.012